Study of the interactions among photosynthesis, respiration and calcification in the scleractinian coral, *Galaxea fascicularis*

Dissertation zur Erlangung des Grades eines Doktors der Naturwissenschaften

-Dr. rer. nat.-

dem Fachbereich Biologie/Chemie der

Universität Bremen

vorgelegt von

Fuad A. Al-Horani

Bremen

Juni 2002

Die vorliegende Arbeit wurde in der Zeit vom November 1999 bis zum Mai 2002 am Max-Planck-Institut für Marine Mikrobiologie in Bremen angefertigt.

1. Gutachter: Prof. Dr. Bo Barker Jørgensen
2. Gutachter: Prof. Dr. Gunter Otto Kirst

Tag des Promotionskolloquiums: 26. Juni 2002

To the soul of my father & to my mother

To my brothers & sister

Preface

The main objectives of this thesis were to study (i) the mechanism of calcification in scleractinian corals and (ii) the role of light and the symbiont in its enhancement. Two main micro-analytical techniques were used. Microsensors for oxygen, calcium and pH were used to characterize the chemical microenvironment on the surface and inside the tissue layers of the coral. The Micro-Imager (a micro-autoradiography technique) was used to study the spatial distribution of calcification on the polyp surface with radioactive tracers. In the thesis, a general introduction was given in the first chapter. The results were presented and discussed in chapters 2-4 followed by a summary section.

This study was funded by the German Federal Ministry of Education and Research (BMBF grants no. 03F0245A) as part of the RSP phase II and the Max Planck Institute for Marine Microbiology which are greatly acknowledged.

I would like to thank the two referees of the thesis; Prof. Dr. Bo Barker Jørgensen and Prof. Dr. Gunter Otto Kirst and the committee members of the thesis defense for their time and efforts.

I am greatly indebted to my supervisors; Dr. Dirk de Beer and Dr. Salim Al-Moghrabi for their efforts and advice during the whole period of my Ph.D. study.

Many thanks to all the people who helped me in one way or another during the period of my study. Of those, I would specially like to thank G. Eickert, A. Eggers, I. Schröder, C. Wigand, U. Witte, A. Gieseke, T. Ferdelman, M. Böttcher, C. Stehning, G. Holst, P. Stief, S. Rousan, N. Finke, H. Jonkers, R. Manasreh, M. Rasheed, R. Abed, C. Schönenberg and all the members of the microsensor group at the Max Planck Institute-Bremen.

Thanks to all the employees of the MPI Bremen, MSS Aqaba and ZMT Bremen.

Fuad A. Al-Horani

June, 2002

Table of Contents

Chapter 1

General Introduction

1. *General Introduction*

1.1. Coral reefs

Coral reefs cover about 15 % of shallow sea floor, and through their roles in marine calcification and fisheries, they are quantitatively significant ecosystem on a global scale (Smith, 1978). They are tropical shallow water ecosystems largely restricted to seas between the latitudes of 30° North and 30° South, where temperature range between 18°C and 30°C (Fig. 1). Exceptional to this, are the cold reefs of *Lophelia pertusa* in the north east Atlantic margin.

There are different types of reefs (Veron, 2000). These are fringing reefs (close to coastlines), barrier reefs (offshore) and atolls (a wall of reefs enclosing a central lagoon). Reefs, which do not conform to these, are called platform reefs. Other types of coral accumulations, found in deep water, which are formed by one or a few species of azooxanthellate corals are called bioherms, e. g. *Lophelia pertusa* reef at depths of 200-1000 m.

The coral reefs are characterized by very high biodiversity with more than hundred thousand species, of which many are not yet identified by science (Hoegh-Guldberg, 1999; Spalding *et al.*, 2001). They are highly productive in tropical seas, in environments described as marine deserts and are critical to the survival of tropical marine ecosystems (Sorokin, 1995; Hoegh-Guldberg, 1999). Productivity may be many thousands of times higher in coral reef areas compared to the open sea (Hatcher, 1988; Hoegh-Guldberg, 1999). Through their role in tourism, fishing, coastline protection and the discovery of new drugs and biochemicals, coral reefs are the source of income for about 15% of the world's population living within 100 Km of coral reef ecosystems (reviewed by Hoegh-Guldberg, 1999). Coral reefs are threatened by many anthropogenic and environmental factors, some of which are the increase in atmospheric CO_2 and the associated decrease in aragonite and calcite saturation states, sea surface temperature, coral diseases, eutrophication and pollution (Smith and Buddemeier, 1992; Brown, 1997; Hodgson, 1999; Leclercq, *et al.,* 2000; Kleypas *et al.,* 2001). In their weakened conditions, coral reefs will be less able to cope with rising sea levels and other anthropogenic stresses, which is expected in the middle of this century (Langdon *et al.,* 2000). By the end of the century, global warming is expected to kill most of the presently existing coral reefs (Pockley, 1999).

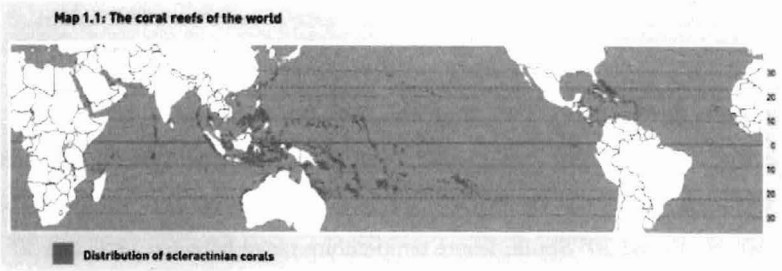

Fig. 1: Distribution of corals in the world's (from Spalding *et al.*, 2001).

1.2. Corals

The most spectacular coral reef organisms are the hermatypic - reef building - corals. Such corals are known for their beautiful shapes and colors. Their skeleton reflects the tissue convolutions in a way that is species characteristic (Barnes and Chalker, 1990). The colors are due to a family of green fluorescent proteins that fluoresce under UV and visible light (Dove *et al.,* 2001).

The corals display mixotrophy in their feeding behavior, i.e. both autotrophy and heterotrophy exist (Porter, 1976; Muscatine *et al.,* 1981; Sorokin, 1995; Ferrier-Pages *et al.*, 1998; Anthony and Fabricius, 2000). Filter feeding and predation on plankton supply the coral with trace metals and other inorganic nutrients. The corals are hermaphrodites or gonochoristic (separate sexes) in their sexual reproduction (Shlesinger and Loya, 1985; Richmond and Hunter, 1990; Shlesinger *et al.*, 1998). They also reproduce asexually by budding. The buds are distributed by currents and waves to other places, where they regrow into new individuals (Sorokin, 1995).

Corals form colonies that vary in their morphologies in different habitats (Goreau and Hartman, 1966; Graus and Macintyre, 1976; Chappell, 1980; McCloskey and Muscatine, 1984; Kaandorp, *et al.*, 1996; Helmuth, *et al.*, 1997). Each colony is built up from small subunits, the

polyps. Each polyp opens to the external environment through a mouth, which in most corals is surrounded by tentacles. In cross section, corals have a thin layer of tissue covering their $CaCO_3$ skeleton. This tissue layer is composed of two epithelia, the oral and aboral epithelium. Each epithelium has two single-cell layers: the ectoderm and endoderm that are separated by non-cellular collagenous layer, the mesoglea. The endodermal cell layers line the coelenteron, the internal body cavity. The oral ectoderm faces the surrounding seawater and the aboral ectoderm, also called calicoblastic layer, covers the skeleton. The adjacent polyps are connected via the coelenteron. Each single polyp produces its skeletal casing, the corallite. The skeletal material between the corallites is the coenosteum (Fig. 2). Scleractinian corals live in an obligate mutualistic symbiotic relationship with multi-species communities of the dinoflagellate *Symbiodinium sp.* (commonly known as zooxanthellae) (Rowan, *et al.*, 1997). The dinoflagellate symbionts are contained in perisymbiotic membranes within the endodermal cells.

1.3. Coral Physiology

The main metabolic processes in corals are photosynthesis (CO_2 consumption and O_2 release), respiration (O_2 consumption and CO_2 release) and the biogeogenic process of calcification (deposition of $CaCO_3$). These processes are interconnected in corals. In the following is a brief description of the three processes.

1.3.1. Photosynthesis

Photosynthesis takes place in plants, algae and some bacteria. The driving force of the process is light, which is transduced into chemical energy in the form of reduced organic compounds.

Two groups of reactions characterize oxygenic photosynthesis: the light and dark reactions. In the light reactions, light energy is captured and oxygen is released as a byproduct from splitting water molecules. The resulting electrons are passed through a series of electron and proton carriers organized between photosystem II and I (PSII and PSI) in the Z-scheme, where ATP and NADPH are produced (Fig. 3). This ATP production is termed non-cyclic photophosphorylation. When $NADP^+$ becomes limiting, electrons are passed between PSI and Cyt b/f complex and ATP is produced. Production of ATP in this way is termed cyclic

photophosphorylation. Neither O_2 nor NADPH is produced in cyclic photophosphorylation. In the dark reactions (also called Calvin-Benson cycle), the ATP and NADPH produced in light reactions are used to fix CO_2. The key enzyme in photosynthetic carbon fixation is ribulose bisphosphate carboxylase-oxygenase (Rubisco). This enzyme is operative in both photosynthetic carbon reduction (PCR) and photorespiratory carbon oxidation (PCO). In the case of PCR pathway, ribulose bisphosphate is carboxylated by Rubisco and organic carbon compounds are produced in the dark reactions. In C-3 plants, glyceraldehyde-3-phosphate (a 3-carbon compound) is first organic carbon compound produced in the dark reactions thus called C-3 pathway. In the case of PCO pathway, Rubisco oxidizes ribulose bisphosphate to phosphoglycolic acid (Marx, 1973; Walker, 1992). Rubisco has a lower affinity to CO_2 than to O_2 (Jordan and Ogren, 1981), high O_2/CO_2 ratios are known to enhance PCO (Laisk and Edwards, 1998). Thus, high CO_2/O_2 ratios are needed to fix CO_2.

In sea, the concentration of dissolved inorganic carbon is about 2.4 mM, mostly present in non-permeable forms, HCO_3^- and CO_3^{2-}. Rubisco uses CO_2 and not HCO_3^- or CO_3^{2-} as a substrate (Hochachka and Somero, 1973; Badger and Price, 1992). Corals and other photosynthetic organisms that live in the sea face a problem in supplying CO_2 to Rubisco. Thus, many marine organisms, including corals, have developed a carbon-concentrating mechanism, through which active HCO_3^- transport elevates CO_2 concentrations around Rubisco to increase the photosynthetic efficiency (Badger and Price, 1992; Benazet-Tambutte *et al.*, 1996; Al-Moghrabi *et al.*, 1996; Allemand *et al.*, 1998; Furla *et al.*, 2000). Membrane-bound H^+-ATPase and carbonic anhydrase (membrane-bound and intracellular) provide another means for the uptake of inorganic carbon from the sea. The two enzymes cooperate in a way where protons pumped by H^+-ATPase are used by carbonic anhydrase for the conversion of HCO_3^- to CO_2, which diffuses into cells and becomes available for photosynthesis (Allemand *et al.*, 1998a; Furla *et al.*, 2000).

1.3.2. Respiration

Gross oxygen consumption in light is a result of at least three processes: oxidative phosphorylation, photorespiration and the Mehler reaction. In oxidative phosphorylation, O_2 is

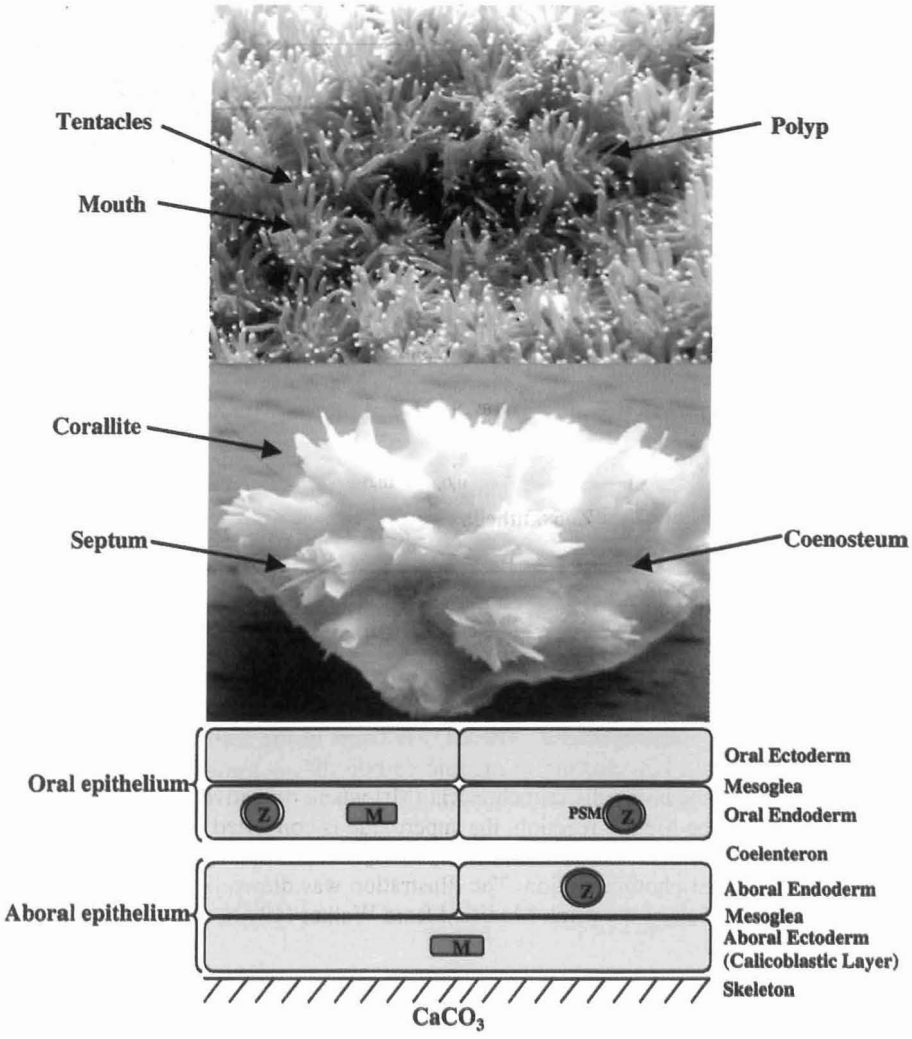

Fig. 2: Morphology and anatomy of scleractinian corals. Polyps (top) and corallites (middle) of *Galaxea fascicularis*. Bottom: schematic drawing of a cross section of the coral tissue layers. Z: zooxanthella, M: Mitochondria, PMS: perisymbiotic membrane.

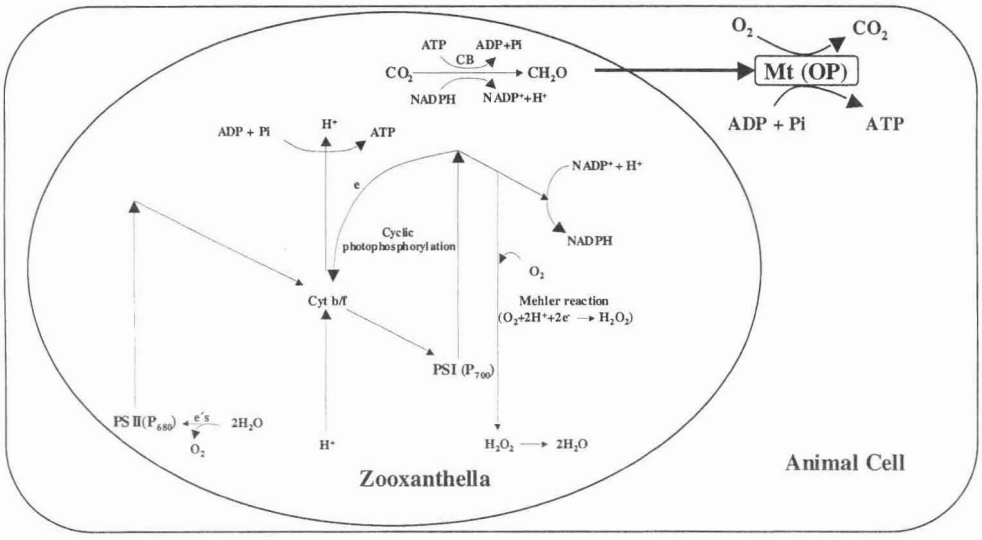

Fig. 3: Simplified drawings of the Z-scheme of PSI and PSII and the associated processes occurring during photosynthesis. The CO_2 is fixed in the Calvin-Benson cycle (CB) with Rubisco as a key enzyme to organic carbon that is partially exported from the zooxanthella to the host cells mitochondria (Mt) where oxidative phosphorylation (OP) takes place. In the Mehler reaction, the superoxide is converted to H_2O_2 by superoxide dismutase, and catalase converts the H_2O_2 to H_2O. The Mehler reaction function as a protection against photoinhibition. The illustration was drawn in a zooxanthella within the endodermal cell of the coral. Modified from Walker (1992).

used as a final electron acceptor during ATP generation in the mitochondria. In photorespiration, the enzyme Rubisco uses O_2 and oxidizes ribulose bisphosphate to phosphoglycolic acid (Marx, 1973; Walker, 1992). In the Mehler reaction, O_2 is reduced to superoxide by the reduced donors associated with PSI (Fig. 3) (Badger *et al.*, 2000). However, photorespiration is not important in coral-inhabiting *Symbiodinium sp.* and the Mehler reaction is considered insignificant in plants following the C-3 carbon-fixation pathway as does *Symbiodinium sp.* (Taylor and Trench, 1986; Streamer *et al.*, 1993; Badger *et al.*, 2000).

Of the three processes, only oxidative phosphorylation produces ATP for the animal metabolism. The Mehler reaction is not a pathway for ATP production and photorespiration is an energy sink rather than an energy producing pathway (Wingler *et al.*, 2000).

1.3.3. Calcification

Many types of minerals are formed by organisms from all the kingdoms and $CaCO_3$ is one of the principal skeletal minerals formed (Simkiss and Wilbur, 1989). The polymorphs of $CaCO_3$, aragonite and calcite, have the widest distribution of all the minerals deposited (Simkiss and Wilbur, 1989). In marine environments, the reef building corals together with coccolithophorids and coralline algae are responsible for over half of the world's $CaCO_3$ production (reviewed by Gattuso and Buddemeier, 2000). In coral reefs, calcification is a major biogeochemical process (Smith, 1978). The gross carbonate production on coral reefs range between 1 and 35 kg $CaCO_3$ m^{-2} yr^{-1} (Barnes and Chalker, 1990). Corals and algae are the major contributors of the coral reef skeletal mass, with foraminiferans and molluscs providing smaller fraction of the total reef mass (Smith, 1978; Barnes and Chalker, 1990).

Calcification is the precipitation of $CaCO_3$ from Ca^{2+} and CO_3^{2-} according to the following reaction:

$$Ca^{2+} + CO_3^{2-} \Longrightarrow CaCO_3$$

The carbonate ion can be formed from carbon dioxide and bicarbonate according to the following reactions:

$$H_2O + CO_2 \Longleftrightarrow H_2CO_3 \Longleftrightarrow H^+ + HCO_3^- \Longleftrightarrow 2H^+ + CO_3^{2-}$$

For calcification to proceed, fluid supersaturation, nucleation, crystal growth and proper machinery are needed. With 10 mM Ca^{2+} and 2.4 mM dissolved inorganic carbon concentrations, tropical seas are supersaturated with respect to aragonite (Gattuso *et al.*, 1998), the form of $CaCO_3$ precipitated by scleractinian corals (Barnes, 1970). The organic matrix that contains glycoproteins, proteins, chitin and phospholipids have the capacity to bind Ca^{2+}, which attracts CO_3^{2-} and nucleation is initiated and the crystal grows within the matrix (Young *et al.* 1971; Mitterer 1978; Constantz and Weiner, 1988; Isa and Okazaki, 1987; Simkiss and Wilbur,

1989; Allemand *et al.* 1998b). In the production process, energy is needed for the transport of ions and the synthesis of an organic matrix (Chalker and Taylor, 1975; Krishnaveni *et al.*, 1989; Allemand *et al.*, 1998b). The enzymes Ca-ATPases and carbonic anhydrase are needed for the transport of Ca^{2+} and inorganic carbon, respectively (Kingsley & Watabe, 1985; Krishnaveni *et al.*, 1989; Ip *et al.*, 1991; Furla *et al.*, 2000).

Many environmental and biological factors influence the rate of calcification. Of these are light, temperature and saturation state are most important. In corals and other symbiotic organisms, the rate of calcification is about 3 times higher in light than in dark (Goreau, 1959; Barnes and Chalker, 1990; see review by Gattuso *et al.*, 1999). Although the exact mechanism behind this discrepancy between light and dark calcification is not well understood, in many cases it was attributed to symbiont photosynthesis (Barnes and Chalker, 1990). The calcification rate is highest at its optimum temperature, which is around 26°C and is significantly decreased when temperature increases 1-2°C above its maximum (Smith and Buddemeier, 1992; McConnaughy, 1994). The saturation state is a primary environmental factor that influence calcification rates in reefs (Langdon *et al.*, 2000). The rate is decreased by decreasing the saturation state of aragonite (Gattuso *et al.*, 1998).

The link between calcification and photosynthesis was established through the observations that many marine calcifiers have the common ability to photosynthesize and that the rate of calcification is increased in the light (Goreau, 1959; Barnes and Chalker, 1990; McConnaughey, 1994; Allemand *et al.*, 1998; Gattuso *et al.*, 1999). A number of conflicting theories were proposed to explain the interactions between photosynthesis and calcification. These include (i) organic carbon fixed by zooxanthellae and the removal of metabolic wastes and crystal poisons is responsible for light enhanced calcification (Goreau, 1959; Simkiss, 1964; Yonge, 1968; Chalker & Taylor, 1975), (ii) calcification generates protons used to assimilate bicarbonate and nutrients (McConnaughey & Whelan, 1997), (iii) calcification does not enhance photosynthesis (Yamashiro, H., 1995; Gattuso, *et al.*, 2000), and (iv) both processes are more efficient in the coexisting system than in the isolated reactions (Suzuki *et al.*, 1995). It is still not known which mechanism is involved and the question remains to be answered (Gattuso *et al.*, 1999).

Of the methods used for estimation of calcification rates are the net weight gain, the alkalinity anomaly technique, staining, radioisotope uptake and most recently calcium microsensors (Goreau, 1959; Smith, 1973; Buddemeier and Kinzie, 1976; Kühl *et al.*, 1995; De Beer *et al.*, 2000).

1.4. Biological sample

Galaxea fascicularis (Linnaeus, 1767) is a widely distributed coral belonging to the family Oculinidea (Fig. 4). It is common in a wide range of habitats and may be a dominant species on inshore fringing reefs (Veron, 2000). It forms small and large colonies in various shapes and colors. The Large colonies exceed 5 m in diameter. The cylindrical corallites vary in size, but are commonly smaller than 10 mm in diameter and have numerous septa (Fig. 2).

G. fascicularis was chosen for the present study because of the relative ease of handling and propagating it in artificial seawater in a closed system aquarium. Furthermore, their relatively big polyps allow detailed measurements with microsensors.

Phylum	Cnidaria
Class	Anthozoa
Subclass	Hexacorallia
Order	Scleractinia
Family	Oculinidea
Genus	*Galaxea*
Species	*fascicularis*

Fig. 4: Taxonomy of the *G. fascicularis* coral.

1.5. General Methods

1.5.1. Microsensors

Microsensors are glass electrodes with minute tip diameter. There are several types of microsensors that have many ecological and physiological applications (Revsbech and Jorgensen, 1986; De Beer, 2000a; Kühl and Revsbech, 2001). Their small tip diameters make them suitable for studying processes occurring in microenvironments with a very high spatial resolution. Microsensors were used in studying the physical and chemical microenvironments of microbial mats, biofilms, and sediments (De Beer, 1998; De Beer, 2000a). Microsensors proved to be useful tools in studying the microenvironments at the surface of symbiotic organisms like corals and foraminiferans (Kühl et al., 1995; Rink et al., 1998; Rink and Kühl, 2000; De Beer, 2000b) and in studying coral diseases (Carlton and Richardson, 1995; Richardson et al., 2001). These studies were limited to coral surfaces. In this study, microsensor technique was used to characterize the calcification mechanism by measurements inside polyps and at the skeleton.

Three types of microsensors were used in this study (Fig. 5). These are: O_2 microsensors (Revsbech and Jorgensen, 1983), LIX calcium and LIX pH microsensors (de Beer *et al.*, 1997; de Beer *et al.*, 2000b). The electrodes were constructed and calibrated according to these authors.

The O_2 microsensors are Clark type electrodes with a gold-coated platinum measuring cathode behind a gas permeable silicon membrane, through which O_2 can diffuse and be reduced at the cathode. The electrode is stable and has a tip size of 5-15μm, a detection limit of 0.1 μM O_2 and a lifetime of longer than a year (Revsbech, 1989).

Gross photosynthesis rate can be measured with fast O_2 electrodes (response time t_{90} < 0.5 s) by the light-dark shift method (Revsbech and Jorgensen, 1983). In this method, the rate of gross O_2 production is measured by the decrease in O_2 concentration in the first second after shutting off the light. For measuring net photosynthesis and respiration rates, the flux is measured by profiling O_2 with depth and using Fick´s first law of diffusion in light gives the net photosynthesis rate and in dark gives the rate of dark respiration. The respiration rate in light is calculated by subtracting the net photosynthesis rate from gross photosynthesis rate.

The LIX Ca^{2+} and pH microsensors are potentiometric electrodes that depend on a potential buildup across a liquid ion exchanger (LIX) membrane with a specific ionophore at the tip of the microsensor (Fig. 5). The tip diameter is 1-10 μm for both electrodes. The detection limit for pH microsensor is 3-11 (De Beer *et al.*, 1997) and 10 μM for calcium electrode in seawater (Amman *et al.*, 1987).

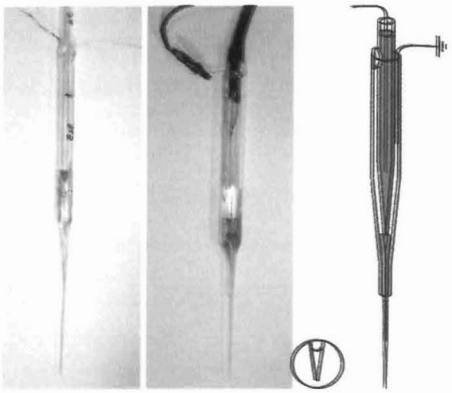

Fig. 5: Photographs and schematic drawing of the microsensors used. Magnified is the tip of the LIX electrodes. LIX: liquid ion exchanger.

1.5.2. Measuring Setup

Coral colonies were placed in a polycarbonate flow cell (0.7 L) for microsensor measurements. Filtered seawater was circulated between the flow cell and a 3 L reservoir at a constant flow rate (420 ml/min). The reservoir was continuously aerated. Motorized micromanipulators fixed on a heavy stand were used to position the electrodes. A halogen light source (KL 1500 Schott Mainz company-Germany) provided a light intensity of 140-μmole

photons m^{-2} s^{-1}. A shutter (Unibliz Electronic) controlled the light entrance. Signals from the millivoltmeter and the picoamperometer were plotted on a strip-chart recorder.

1.5.3. The Micro Imager

The Micro-Imager (Fig. 6) is a new technology that allows quantitative real-time analysis of radiolabelled samples with a high spatial resolution and high detection sensitivity. In this machine, the light generated by the ionizing radiation (α, β, γ) in a thin solid scintillator is amplified by an image intensifier, consisting of a few million 10 μm quartz capillaries. The amplified light is then transmitted to a high resolution charge-coupled device (CCD) camera connected to a PC equipped with software for the analysis of such data. The sensitive area is 2.4 cm x 3.2 cm and the measuring time depends on the radioactivity in the sample, ranging from minutes to hours.

The Micro-Imager is suitable for imaging radio- and luminescence labeled tissues, bacteria and cell cultures, and in this study for coral slices.

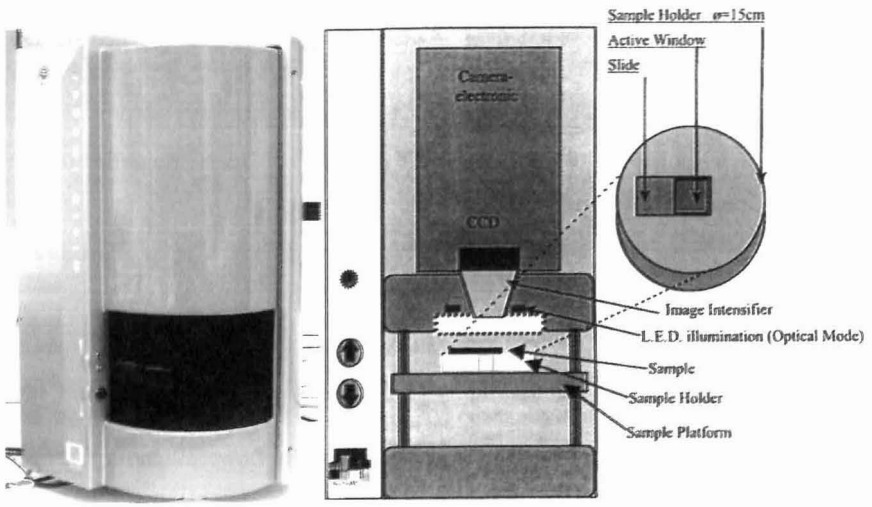

Fig. 6: photograph (left) and schematic representation (right) of the Micro-Imager.

1.6. Thesis Outline

The main objectives that were addressed in this thesis are: (1) to study the mechanism of calcification in scleractinian corals, (2) to study the mechanism of light enhancement of calcification and (3) to investigate the interactions among photosynthesis, respiration and calcification in corals.

Because carbon is a common substrate and product of photosynthesis, respiration and calcification in corals, the first study (chapter 2) was dedicated toward studying the sources of carbon for the three processes. This study revealed an internal cycle of carbon between photosynthesis and respiration and that carbon is pooled within the symbiotic unit (the symbiont and the animal host). I observed that carbon from the different pools (e.g. tissue, skeleton, photosynthates, and the dissolved organic and inorganic carbon in seawater and in coral) could exchange. Thus it is very difficult to follow the fate of carbon from one pool. The main output of the carbon cycle is energy, which fuels the energy requiring processes in the animal. Furthermore, both inorganic carbon and organic carbon from the surrounding seawater are used as external carbon sources.

The second study (chapter 3) focused on studying of the mechanism of calcification and the role of light in its enhancement. Because the site of calcification is the space between the calicoblastic layer and the skeleton, a new approach was developed to study conditions prevailing in that specific site. This study indicated that there is a Ca^{2+}-H^{+}-ATPase enzyme on the calicoblastic layer that pump calcium to the skeleton site and removes protons away, creating a microenvironment suitable for calcification at high rates in the light. This enzyme is triggered by light, while the ATP required for the enzyme function is supplied by the carbon cycle between photosynthesis and respiration.

In the last study (chapter 4), the heterogeneous polyp surface of the coral was studied physiologically with a high spatial resolution using microsensors and micro-autoradiography techniques. The distribution of photosynthesis and calcification on the polyp surface was analyzed. It turns out that the higher rates of calcification are supported by higher rates of photosynthesis in the adjacent polyp parts. Furthermore, a new approach was used to distinguish

between dark calcification and isotopic exchange where it was possible to estimate both processes in corals using the radioactive tracer method.

References

1. Allemand, D., Furla, P., Benazet-Tambutte, S. (1998a). Mechanisms of carbon acquisition for endosymbiont photosynthesis in Anthozoa. Can. J. Bot. 76, 925-941.

2. Allemand, D., Tambutte, E., Girard, J. –P., Jaubert, J. (1998b). Organic matrix synthesis in the scleractinian coral *Stylophora pistillata*: role in biomineralization and potential target of the organotin tributyltin. J. Exp. Biol. 201, 2001-2009.

3. Al-Moghrabi, S., Goiran, C., Allemand, D., Speziale, N., Jaubert, J. (1996). Inorganic carbon uptake for photosynthesis by the symbiotic coral-dinoflagellate association II. Mechanisms for bicarbonate uptake. J. Exp. Mar. Biol. Ecol. 199, 227-248.

4. Amman, D., Bührer, T., Schefer, U., Müller, M., Simon, W. (1987). Intracellular neural carrier based Ca^{2+} microsensor with sub-nanomolar detection limit. Pflügers Arch. 409, 223-228.

5. Anthony, K. R. N., Fabricius, K. E. (2000). Shifting roles of heterotrophy and autotrophy in coral energetics under varying turbidity. J. Exp. Mar. Biol. Ecol. 252, 221-253.

6. Badger, M. R., Price, G. D. (1992). The CO_2 concentrating mechanism in cyanobacteria and microalgae. Physiol. Plant. 84,606-615.

7. Badger, M. R., von Caemmerer, S., Ruuska, S., Nakano, H. (2000). Electron flow to oxygen in higher plants and algae: rates and control of direct photoreduction (Mehler reaction) and Rubisco oxygenase. Phil. T. R. S. Lond. B 355(1402), 1433-1445.

8. Barnes, D. J. (1970). Coral skeletons: an explanation of their growth and structure. Science. 170, 1305-1308.

9. Barnes, D. J., Chalker, B. E. (1990). Calcification and photosynthesis in reef-building corals and algae. In Z. Dubinsky (ed.), Coral reefs, pp. 109-131. Elsevier, Amsterdam.

10. Benazet-Tambutte, S., Allemand, D., Jaubert, J. (1996). Permeability of the oral epithelial layers in cnidarians. Mar. Biol. 126, 43-53.

11. Brown, B. E. (1997). Coral bleaching: causes and consequences. Coral Reefs. 16, S129-S138.

12. Buddemeier, R. W., Kinzie, R. A. (1976). Coral growth. Oceanogr. Mar. Biol. Ann. Rev. 183-225.

13. Carlton, R. G., Richardson, L. L. (1995). Oxygen and sulfide dynamics in a horizontally migrating cyanobacterial mat- black band disease of corals. FEMS Mic. Ecol. 18 (2), 155-162.

14. Chalker, B. E., Taylor, D. L. (1975). Light-enhanced calcification, and the role of oxidative phosphorylation in calcification of the coral *Acropora cervicornis*. Proc. R. Soc. Lond. B. 190, 323-331.

15. Chappell, J. (1980). Coral morphology, diversity and reef growth. Nature 286, 249-252.

16. Constantz, B., Weiner, S. (1988). Acidic macromolecules associated with mineral phase of scleractinian coral skeletons. J. Exp. Zool. 248, 253-258.

17. De Beer, D. (1998). Use of micro-electrodes to measure in situ microbial activities in biofilms, sediments and microbial mats. In Molecular Microbial Ecology Manual (eds. Akkermans, A. D. L., van Elsas, J. D., de Bruyn, F. J.). Pp. 8.1.3.1-23. Kluwer Acad. Press. Netherlands.

18. De Beer, D. (2000a). Potentiometric microsensors for *in situ* measurements in aquatic environments, p. 161-194. In J. Buffle and G. Horvani (ed.), In Situ Monitoring of aquatic systems: chemical analysis and speciation. John Wiley & Sons Ltd.

19. De Beer, D., Kühl, M., Stambler, N., Vaki, L. (2000b). A microsensor study of light enhanced Ca^{2+} uptake and photosynthesis in the reef-building hermatypic coral *Favia* sp. Mar. Ecol. Prog. Ser. 194, 75-85.

20. De Beer, D., Schramm, A., Santegoeds, C., Kühl, M. (1997). A nitrite microsensor for profiling environmental biofilms. App. Env. Microbiol. Mar. 63, 973-977.

21. Dove, S. G., Hoegh-guldberg, O., Ranganathan, S. (2001). Major colour patterns of reef-building corals are due to a family of GFP-like proteins. Coral Reefs. 19, 197-204.

22. Ferrier-Pages, C., Allemand, D., Gattuso, J. –P., Jaubert, J. (1998). Microheterotrophy in the zooxanthellate coral *Stylophora pistillata*: effects of light and ciliate density. Limnol. Oceanogr. 43(7), 1639-1648.

23. Frankignoulle, M., Canon, C., Gattuso, J. –P. (1994). Marine calcification as a source of carbon dioxide: positive feedback of increasing atmospheric CO_2. Limnol. Oceanogr. 39(2), 458-462.

24. Furla, P., Allemand, D., Orsenigo, M. -N., (2000). Involvement of H^+-ATPase and carbonic anhydrase in inorganic carbon uptake for endosymbiont photosynthesis. Am. J. Physiol. 278, R870-R881.

25. Gattuso, J. –P., Allemand, D., Frankignoulle, M. (1999). Photosynthesis and calcification at cellular, organismal and community levels in coral reefs: a review on interactions and control by carbonate chemistry. Amer. Zool. 39, 160-183.

26. Gattuso, J. –P., Buddemeier, R. W. (2000). Calcification and CO_2. Nature 407, 311-313.

27. Gattuso, J. –P., Frankignoulle, M., Bourge, I., Romaine, S., Buddemeier, R.W. (1998). Effect of calcium carbonate saturation of seawater on coral calcification. Global and Planetary Change. 18, 37-46.

28. Goreau, T. F. (1959). The physiology of skeleton formation in corals. I. A method for measuring the rate of calcium deposition by corals under different conditions. Biol. Bull. 116, 59-75.

29. Goreau, T. F., Hartman, W. D. (1966). Sponge: Effect on the form of reef corals. Science 151, 343-344.

30. Graus, R. R., Macintyre, I. G. (1976). Light control of growth form in colonial reef corals: computer simulation. Science 193, 895-897.

31. Hatcher, B. G. (1988). Coral reef primary productivity: A beggar's banquet. Trends in Ecol. Evol. 3, 106-111.

32. Helmuth, B. S. T., Sebens, K. P., Daniel, T. L. (1997). Morphological variation in coral aggregations: branch spacing and mass flux to coral tissues. J. Exp. Mar. Biol. Ecol. 209, 233-259.

33. Hochachka, P. W., Somero, G. N. (1973). Strategies of biochemical adaptation. E. B. Saunders Company. Philadelphia.

34. Hodgson, G. (1999). A global assessment of human effects on coral reefs. Mar. Poll. Bull. 38, 345-355.

35. Hoegh-Guldberg, O. (1999). Climate change, coral bleaching and the future of the world's coral reefs. Mar. Freshwater Res. 50, 839-866.

36. Ip, Y. K., Lim, A. L. L., Lim, R. W. L. (1991). Some properties of calcium-activated adenosine triphosphatase from the hermatypic coral *Galaxea fascicularis*. Mar. Biol. Vol. 111, pp. 191-197.

37. Isa, Y., Okazaki, M. (1987). Some observations on the calcium binding phospholipid from scleractinian coral skeletons. Comp. Biochem. Physiol. 87B, 507-512.

38. Jordan, D. B., Ogren, W. L. (1981). Species variation in the specificity of ribulose bisphosphate carboxylase/oxygenase. Nature 291, 513-515.

39. Kaandorp, J. A., Lowe, C. P., Frenkel, D., Sloot, P. M. A. (1996). Effect of nutrition and flow on coral morphology. Physical Rev. Lett. 77 (11), 2328-2331.

40. Kingsley, R. J., Watabe, N., (1987). Role of carbonic anhydrase in calcification in the gorgonian *Leptogorgia virgulata*. J. Exp. Zool. 241, 171-180.

41. Kleypas, J. A., Buddemeier, R. W., Gattuso, J. –P. (2001). The future of coral reefs in an age of global change. Int. J. Earth Sciences 90, 426-437.

42. Krishnaveni, P., Chou, L. M., Ip, Y. K. (1989). Deposition of calcium ($^{45}Ca^{2+}$) in the coral, *Galaxea fascicularis*. Comp. Biochem. Physiol. 94A, 509-513.

43. Kühl, M., Cohen, Y., Dalsgaard, T., Jorgensen, B. B., Revsbech, N. P. (1995). Microenvironment and photosynthesis of zooxanthellae in scleractinian corals studied with microsensors for O_2, pH and light. Mar. Ecol. Prog. Ser. 117, 159-172.

44. Kühl, M., Revsbech, N. P. (2001). Biogeochemical microsensors for boundary layer studies, p. 180-210. In B. Boudreau and B. Jorgensen (ed.), The benthic boundary layer. Oxford University Press, Oxford.

45. Laisk, A., Edwards, G. E. (1998). Oxygen and electron flow in C-4 photosynthesis: Mehler reaction, photorespiration and CO_2 concentration in the bundle sheath. PLANTA 205(4), 632-645.

46. Langdon, C., Takahashi, T., Sweeney, C., Chipman, D., Goddard, J., Marubini, F., Aceves, H., Barnett, H., Atkinson, M. J. (2000). Effect of calcium carbonate Saturation State on the calcification rate of an experimental coral reef. Global Biogeochemical Cycles 14, 639-654.

47. Langdone, C., Takahashi, T., Sweeney, C., Chipman, D., Goddard, J., Marubini, F., Aceves, H., Barnett, H., Atkinson, M. J. (2000). Effect of calcium carbonate saturation state on the calcification rate of an experimental coral reef. Global Biogeochemical cycles. 14, 639-654.

48. Leclercq, N., Gattuso, J. –P., Jaubert, J. (2000). CO_2 partial pressure controls the calcification rate of a coral community. Global Change Biology. 6, 329-334.

49. Marx, J. L. (1973). Photorespiration: key to increasing plant productivity? Science 179, 365-367.

50. McCloskey, L. R., Muscatine, L. (1984). Production and respiration in the Red Sea coral *Stylophora pistillata* as a function of depth. Proc. R. Soc. Lond. B. 222, 215-230.

51. McConnaughey, T. A. (1994). Calcification, photosynthesis, and global carbon cycles. Bull. Inst. Oceanogr. (Monaco). 137-161.

52. McConnaughey, T. A., LaBaugh, J. W., Rosenberry, D. O., Reddy, M. M., Schuster, P. F., Carter, V. (1994). Carbon budget for a groundwater-fed lake: calcification supports summer photosynthesis. Limnol. Oceanogr. 39(6), 1319-1332.

53. McConnaughey, T. A., Whelan, J. F. (1997). Calcification generates protons for nutrient and bicarbonate uptake. Earth Sci. Rev. 42, 95-117.

54. Mitterer, R. M. (1978). Amino acid composition and metal binding capability of the skeletal protein of corals. Bull. Mar. Sci. 28, 173-180.

55. Muscatine, L. and D´Elia, C. F. (1978). The uptake, retention, and release of ammonium by reef corals. Limnol. Oceanogr. 23(4), 725-734.

56. Muscatine, L., McCloskey, L. R., Marian, R. E. (1981). Estimating the daily contribution of carbon from zooxanthellae to coral animal respiration. Limnol. Oceangr. 26(4), 601-611.

57. Pockley, P. (1999). Global warming "could kill most coral reefs by 2100". Nature 400, 98.

58. Porter, J. W. (1976). Autotrophy, heterotrophy, and resource partitioning in Caribbean reef building corals. Am. Nat. 110, 731-742.

59. Revsbech, N. P. (1989). An oxygen microsensor with a guard cathode. Limnol. Oceanogr. 34 (2), 474-478.

60. Revsbech, N. P., Jorgensen, B. B. (1983). Photosynthesis of benthic microflora measured with high spatial resolution by the oxygen microprofile method. Limnol. Oceanogr. 28(4), 749-756.

61. Revsbech, N. P., Jorgensen, B. B. (1986). Microelectrodes: Their use in microbial ecology, p. 293-352. In K. C. Marshall (ed.), Advances in Microbial Ecology, Vol. 9. Plenum Press, New York.

62. Richardson, L. L., Smith, G. W., Ritchie, K. B., Carlton, R. G. (2001). Integrating microbiological, microsensor, molecular, and physiologic techniques in the study of coral disease pathogenesis. Hydrobiologia 460, 71-89.

63. Richmond, R. H., Hunter, C. L. (1990). Reproduction and recruitment of corals: comparisons among the Caribbean, the tropical Pacific, and the Red Sea. Mar. Ecol. Prog. Ser. 60, 185-203.

64. Rink, S. K., Kühl, M. (2000). Microsensor studies of photosynthesis and respiration in larger foraminifera. I The physico-chemical microenvironment of *Marginopora vertebralis*, *Amphistigena lobifera* and *Amphisorus hemprichii*.Mar. Biol. 137, 473-486.

65. Rink, S., Kühl, M., Bijma, J., Spero, H. J. (1998). Microsensor studies of photosynthesis and respiration in the symbiotic foraminifer *Orbulina universa*. Mar. Biol. 131, 583-595.

66. Rowan, R., Knowlton, N., Baker, A., Jara, J. (1997). Landscape ecology of algal symbionts creates variation in episodes of coral bleaching. Nature 388, 265-269.

67. Shlesinger, Y., Goulet, T. L. Loya, Y. (1998). Reproductive patterns of scleractinian corals in the northern Red Sea. Mar. Biol. 132, 691-701.

68. Shlesinger, Y., Loya, Y. (1985). Coral community reproductive patterns: Red Sea versus the Great Barrier Reef. Science 228, 1333-1335.

69. Simkiss, K. (1964). Phosphates as crystal poisons of calcification. Biol. Rev. 39, 487-505.

70. Simkiss, K., Wilbur, K. M. (1989). Biomineralization: Cell biology and mineral deposition. Academic press, Inc. UK.

71. Smith, S. V. (1973). Carbon dioxide dynamics: A record of organic carbon production, respiration, and calcification in the Eniwetok reef flat community. Limnol. Oceanogr. 18, 106-120.

72. Smith, S. V. (1978). Coral reef area and the contributions of reefs to processes of the world's oceans. Nature 273, 225-226.

73. Smith, S. V., Buddemeier, R. W. (1992). Global change and coral reef ecosystems. Ann. Rev. Ecol. Syst. 23, 89-118.

74. Sorokin, Y. I. (1995). Coral reef ecology. Springer- verlag, Berlin, Germany.

75. Streamer, M., McNeil, Y. R., Yellowlees, D. (1993). Photosynthetic carbon dioxide fixation in zooxanthellae. Mar. Biol. 115(2), 195-198.

76. Suzuki, A., Nakamori, T., Kayanne, H. (1995). The mechanism of production enhancement on coral reef carbonate systems: model and empirical results. Sed. Geol. 99, 259-280.

77. Tambutte, E., Allemand, D., Mueller, E., Jaubert, J. (1996). A compartmental approach to the mechanisms of calcification in hermatypic corals. J. Exp. Biol. 199, 1029-1041.

78. Tayler, E. M., Trench, R. K. (1986). Activities of enzymes in B-carboxylation reactions and of catalase in cell-free preparations from the symbiotic dinoflagellates Symbiodinium spp. from a coral, a clam, a zoanthid and two sea anemones. Proc. R. Soc. Lond. B. 228, 483-492.

79. Veron, J. (2000). Corals of the world. (Ed. Stafford-Smith, M.). Australian Institute of Marine Science and CRR Qld Pty Ltd.

80. Walker, D. (1992). Excited leaves. New Phytol. 121, 325-345.

81. Wingler, A., Lea, P. J., Quick, W. P., Leegood, R. C. (2000). Photorespiration: metabolic pathways and their role in stress protection. Phil. T. R. Soc. Lond. B-Biol. Sci. 355(1402), 1517-1529.

82. Yamashiro, H. (1995). The effect of HEBP, an inhibitor of mineral deposition, upon photosynthesis and calcification in the scleractinian coral, *Stylophora pistillata*. J. Exp. Mar. Biol. Ecol. 191, 57-63.

83. Yonge, C. M. (1968). Living corals. Proc. R. Soc. Lond. Ser. B. 169, 329-344.

84. Young, S. D., O´connor, J. D., Muscatine, L. (1971). Organic material from scleractinian coral skeletons-II. Incorporation of ^{14}C into protein, Chitin and lipid. Comp. Biochem. Physiol. 40B, 945-958.

Chapter 2

Microsensor Study of Photosynthesis and Calcification in the Scleractinian Coral, *Galaxea fascicularis*: active internal carbon cycle

Manuscript submitted for publication in J. Experimental Marine Biology and Ecology

Microsensor Study of Photosynthesis and Calcification in the Scleractinian Coral, *Galaxea fascicularis*: active internal carbon cycle

Fuad A. Al-Horani[1, 2], Salim M. Al-Moghrabi[2], Dirk de Beer[1]

1. Max-Planck Institute for Marine Microbiology, Celsiusstrasse1, D-28359 Bremen, Germany
2. Marine Science station, P. O. Box (195), Aqaba, 77110 Jordan

Abstract

Sources of inorganic carbon (Ci) for photosynthesis and calcification and the mechanisms involved in their uptake in scleractinian corals were investigated in microcolonies of *Galaxea fascicularis*. Direct measurements of Ca^{2+}, pH and O_2 on the surface and inside the polyp's coelenteron were done with microsensors. Gross photosynthesis (Pg) and net photosynthesis (Pn) were measured on the surface. Light respiration (LR) was calculated from Pg and Pn. The effect of light/dark and dark/light switches on Ca^{2+} and pH dynamics on the surface and inside the coelenteron were followed. To evaluate the different sources of Ci for photosynthesis and calcification, Ci-free seawater and 6-Ethoxyzolamide (EZ) and Acetazolamide (AZ), inhibitors for carbonic anhydrase (CA) were used.

In normal seawater, Pg was seven times higher than Pn, the LR was ca. 80-90% of the Pg. Thus most O_2 produced in Pg is immediately consumed in respiration, indicating the presence of a highly active internal C-cycle. As the internal C-cycle is highly active, a large part of the Ci for calcification will have past through the metabolisms of the symbiont. The high LR provides ATP for energy requiring processes in light. Illumination increased Ca^{2+} uptake and pH on the surface and inside the coelenteron.

In Ci-free seawater, Pg decreased by 14%, indicating that most of the photosynthetic Ci can temporarily be supplied from internal sources. The initial decalcification, observed directly upon the switch to Ci-free seawater, showed that the different Ca-pools in the coral are dynamic. Part of the Pg in Ci-free seawater may depend on this decalcification. The inhibition of CA decreased Pg by 30%, while it increased the concentration of Ca^{2+} causing a decrease in calcium precipitation. This effect of CA inhibition on photosynthesis and calcification demonstrated that both processes are in need for the enzyme. The pH on the surface and inside the coelenteron decreased upon EZ addition.

Ci for photosynthesis and calcification can come from seawater (free Ci) including internal C-cycle or by feeding on plankton and respiration of its organic carbon content. These sources form a common carbon pool, which is used for the different processes.

Three localities of CA were defined. One on the surface facing seawater and one on endodermal cells facing the coelenteron, while the third is intracellular.

Key words: coral; *Galaxea fascicularis*; photosynthesis; respiration; calcification; carbon cycle; inorganic carbon; microsensors.

1. Introduction:

Scleractinian corals live in tropical seas, an oligotrophic alkaline environment, characterized by high calcium and carbonate saturation states (Gattuso *et al.*, 1999). They live in a symbiotic relationship with the dinoflagellate *Symbiodinium sp.* (zooxanthellae). Due to light limitation in deep water, corals are more successful in shallow water (Smith, 1978).

Coral polyps look like a bag. The outer walls are made up of two single-celled epithelia, the ectoderm and the endoderm separated by mesoglea. Zooxanthellae are surrounded by a perisymbiotic membrane and located into the endodermal cells. The oral ectoderm is in direct contact with the surrounding seawater. The oral and aboral endoderm faces the coelenteron, which is connected with external seawater through the mouth (Barnes and Chalker, 1990). The aboral ectoderm (known as calicoblastic layer) faces the $CaCO_3$ skeleton and creates an isolated environment suitable for calcification (Al-Horani *et al.*, in preparation) (Fig. 1).

Calcification by the animal host and photosynthesis by zooxanthellae are processes that need continuous supply of inorganic carbon (Ci). The Ci used for photosynthesis includes CO_2 produced internally by metabolic respiration of photosynthates (i.e. internal cycle) or consumption of plankton, Ci from external seawater and/or CO_2 generated by calcification. Metabolic respiration and external seawater are possible sources of Ci for calcification (Pears, 1970; Goreau, 1977).

The 2.4 mM of Ci in seawater comprises HCO_3^- (ca. 90%), CO_3^{2-} (ca. 10%) and CO_2 (<1%). The zooxanthellae and the calicoblastic layer (calcifying layer) are not in direct

contact with seawater. Biological membranes are not permeable to HCO_3^- and CO_3^{2-}, while CO_2 is present in insignificant amounts in seawater. Thus Ci may be limiting for coral growth (Marubini and Thake, 1999) and zooxanthellae in hospite (Goiran *et al.*, 1996;

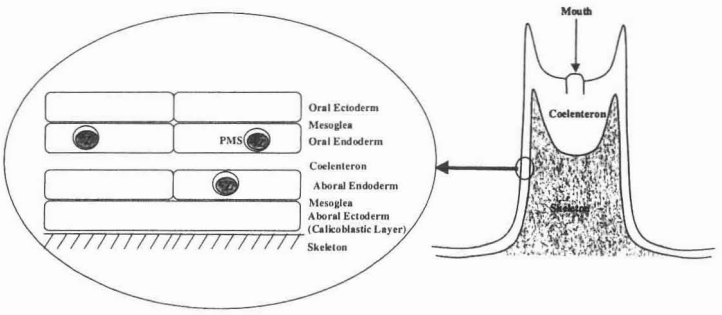

Fig. 1: Schematic representation of the compartmentalized structure of the coral showing longitudinal section (right) and a cross section (magnified) of the polyp. Z: zooxanthellae, PMS: perisymbiotic membrane.

Laggat *et al.*, 2000). Ribulose bisphosphate carboxylase-oxygenase (Rubisco) uses CO_2 and not HCO_3^- as a substrate (Hochachka and Somero, 1973; Badger and Price, 1992) and has a low affinity for CO_2 (Jordan and Ogren, 1981). Many marine organisms have a carbon-concentrating mechanism (CCM) to increase their photosynthetic efficiency (Allemand *et al.*, 1998a). CCM was found in cyanobacteria and microalgae (Badger and Price, 1992), corals (Al-Moghrabi *et al.*, 1996; Furla *et al.*, 2000b) and sea anemone (Benazet-Tambutte *et al.*, 1996). Components of the CCM include active uptake systems for HCO_3^- (Al-Moghrabi *et al.*, 1996) and intracellular CA to catalyse the interconversion between CO_2 and HCO_3^- at the active site of Rubisco. Membrane bound H^+-ATPase and CA are needed to convert seawater HCO_3^- into CO_2 which diffuses into cells (Furla *et al.*, 2000a).

The current study aimed at investigating the different sources of Ci (both internal and external). Previously, different methodological approaches have been used to study Ci supply for photosynthesis and calcification (for review see Allemand *et al.*, 1998a). The use of microsensors is a new method. It enabled spatial and temporal resolution for biological processes occurring in different localities and compartments of the coral polyp and allows the measurement of Pg and Pn. Microsensors for O_2, Ca^{2+} and pH were positioned on the

surface of the oral ectoderm and/or in the coelenteron of the polyps. The Ca^{2+} and pH dynamics were followed upon light/dark and dark/light switches. Furthermore, the effects of inhibitors for CA and Ci-free seawater were evaluated. The Pg, Pn and LR were measured under the different experimental conditions.

2. Materials and Methods:

2.1. Coral samples: *G. fascicularis* colonies were collected by SCUBA diving from a 5-m depth south to the Marine Science Station, Aqaba-Jordan. The collected colonies were immediately transferred to a $2m^3$ aquarium supplied with normal seawater and illuminated with HQI-lamp similar to the natural light (12hr: 12hr light-dark cycle). The colonies were fragmented into smaller microcolonies and left for at least two weeks to acclimatize to the aquarium conditions before use.

2.2. Seawater: Seawater was filtered through 0.45μm Filters. The water had 40 ‰ salinity, pH 8.2-8.3 and ambient temperature of 20-21°C. Ci-free seawater was prepared by lowering the pH of the filtered seawater to ca. 3.5 by 1 N HCl and flushed extensively with N_2-gas to get rid of the CO_2. Then the pH was adjusted to 8.2 by 1N NaOH solution.

2.3. Inhibitors: 6-Ethoxyzolamide (EZ) an inhibitor of CA that penetrate cells was dissolved in dimethylsulfoxide (DMSO) and added to a final concentration of 1 mM. The impermeable CA inhibitor, Acetazolamide (AZ) was prepared the same way and added to a final concentration of 600μM. The final concentration of DMSO was 1 ‰.

2.4. Microsensors: Ca^{2+} microsensors (de Beer *et al.*, 2000), Clark type O_2 electrodes (Revsbech and Jorgensen, 1983) and LIX pH microsensors (de Beer *et al.*, 1997) were constructed and calibrated as described. Positioning of the electrodes on the surface of *G. fascicularis* polyps followed the way described in (Kühl *et al.*, 1995). Microsensors (ca. 5μm diameter tip) were inserted in the mouth opening into the coelenteron to track dynamics of Ca^{2+} and pH. Profiles of O_2 in light were used to calculate Pn using Fick`s first low of diffusion, assuming 100μm tissue thickness. Pg was measured according to the method described in (Kühl *et al.*, 1995) again assuming 100μm tissue thickness. LR was calculated by subtracting Pn from Pg. Because of the physiological differences between individual coral colonies and between polyps in the same individual colony and

the fact that polyp surface is heterogeneous, a control measurement was done for each experiment on the same polyp and position of the electrode.

2.5. Experimental set-up: Coral colonies were placed in a polycarbonate flow cell for microsensor measurements. Filtered seawater was circulated between the flow cell and a 3L reservoir at a constant flow rate (420 ml/min). The reservoir was continuously aerated. Motorized micromanipulators fixed on a heavy stand were used to position the electrodes. A halogen light source (KL 1500 Schott Mainz company-Germany) provided a light intensity of 140-μmole photons.m^{-2}.s^{-1}. A shutter (Unibliz Electronic) controlled the light entrance. Signals from the millivoltmeter and the picoamperometer were plotted on a strip-chart recorder.

3. Results:

3.1. Measurements in normal seawater

Rates of gross photosynthesis (Pg) light respiration (LR) and net photosynthesis (Pn) in *G. fascicularis* polyps are shown in Fig. 2. The Pg/Pn ratio is ca. 7; thus most of the oxygen produced by zooxanthellae is immediately consumed by respiration. Only small fraction of the photosynthetically produced oxygen (ca. 10-20%) is released to seawater, while LR consumes 80-90%.

The effects of light/dark and dark/light switches on Ca^{2+} and pH dynamics on the surface and inside the coelenteron of the polyp are shown in Fig. 3. Ca^{2+} concentration decreased in response to illumination and increased in response to darkening in both compartments. In response to illumination, a fast initial decrease of Ca^{2+} that lasted for few minutes and followed by a slower decrease was observed in the two compartments. The inverse happened in response to darkening. In light, the Ca^{2+} concentration on the surface (ca. 9.9 mM) is lower than in seawater (10.0 mM), and even lower inside the coelenteron (ca. 9.7 mM), forming a downward Ca^{2+}-gradient from seawater to the coelenteron. In the dark, the situation is inverted. Ca^{2+} dynamics inside the coelenteron are less regular than surface dynamics.

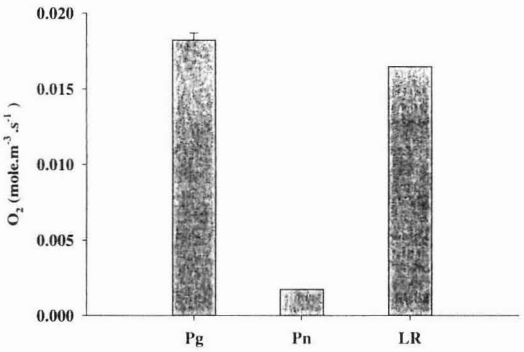

Fig. 2: Rates of gross photosynthesis (Pg) light respiration (LR) and net photosynthesis (Pn) in *G. fascicularis* polyps in normal seawater.

The pH on the surface and inside the coelenteron increased in response to illumination to values of 8.74 and 8.46, respectively, and decreased in response to darkening to values of 7.93 and 8.18, respectively. In light, the surface pH was higher than inside the coelenteron. The surface pH changed faster after illumination and/or darkening compared to pH change inside the coelenteron. This change is fast in the first few minutes and became slow in the following period. In the coelenteron, the response to light/dark switches is not instant. A lag period characterized by acidification followed by a slower alkalization was observed in the coelenteron upon illumination (Fig. 3).

3.2. Measurements in Ci-free seawater

Exclusion of Ci from the surrounding seawater decreased Pg by ca. 14%. This reduction in Pg was accompanied by LR reduction, while Pn was not affected under this experimental condition (Fig. 4). Ca^{2+} level was 0.2-0.4 mM higher on the surface and 0.4-1.0 mM higher inside the coelenteron when compared to the control dynamics in the two compartments (Fig. 5). The initial Ca^{2+} concentrations were ca. 10.3 and10.8 mM on the surface and inside the coelenteron, respectively (Fig. 5C&D), while the concentrations were less than 10 mM in the two compartments in normal seawater (Fig. 5A&B). This indicates that the skeleton dissolved under such conditions at least for short period of time (<10min.), and that Ca^{2+} leaked from the skeleton into the coelenteron and diffused to the surface of the polyp. The high concentrations of Ca^{2+} on the surface and inside the coelenteron gradually

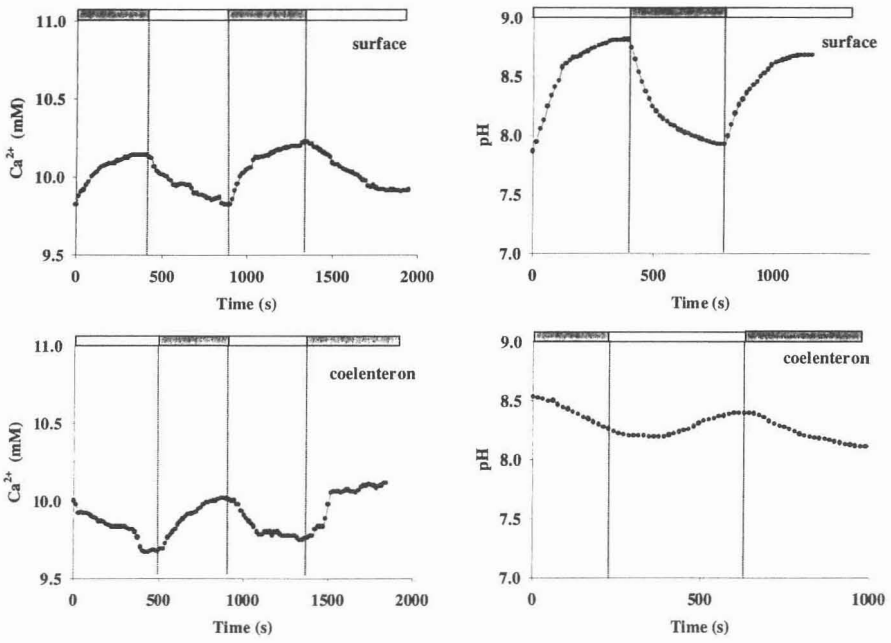

Fig. 3: Dynamics of Ca^{2+} and pH on the surface and inside the coelenteron of *G. fascicularis* polyps. Dark bars indicate dark period and light bars indicate illumination.

decreased indicating a decrease of Ca^{2+} efflux and decalcification (Fig. 5C&D).

The surface and the coelenteron became slightly acidified in Ci-free seawater (Fig. 6C&D). The average surface pH in light decreased from 8.51 in normal seawater to 8.24 in Ci-free seawater. In the coelenteron, the average pH decreased from 8.46 to 8.05 (Fig. 6). Another noticeable difference observed in the absence of Ci is the fast and abrupt alkalization of the coelenteron upon switching the light on (Fig.6D).

3.3. Effect of CA inhibition

The use of permeable (EZ) and impermeable (AZ) inhibitors of CA inhibited Pg with 30% (Fig. 7). EZ completely inhibited Pn, while no effect on Pn was observed with AZ addition. EZ had no effect on LR, while AZ reduced LR with ca. 30% (Fig. 7).

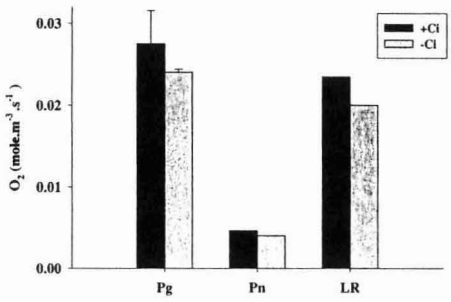

Fig. 4: Effect of Ci removal from seawater on Pg, Pn and LR in *G. fascicularis*.

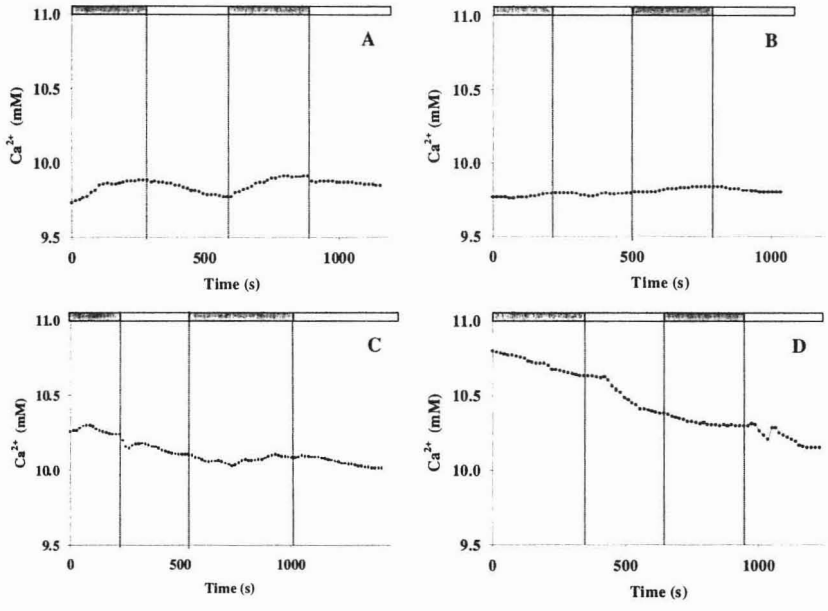

Fig. 5: Effect of Ci removal from seawater on Ca^{2+} dynamics on the surface and inside the coelenteron of *G. fascicularis* polyps. Ca^{2+} dynamics on surface (A) and inside coelenteron (B) in normal seawater. Ca^{2+} dynamics on surface (C) and In Ci-free seawater, decalcification was observed inside coelenteron (D) in Ci-free seawater. Dark bars indicate dark period and light bars indicate illumination.

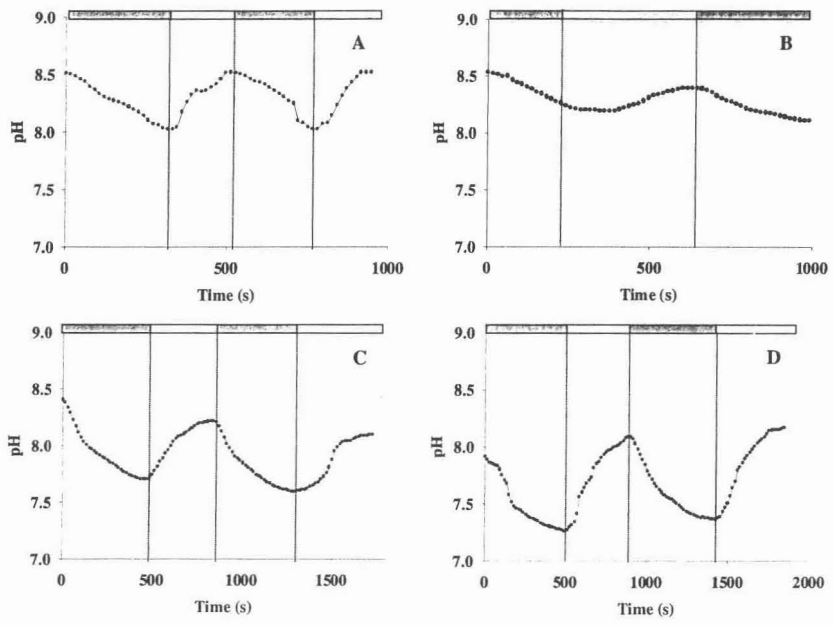

Fig. 6: Effect of Ci removal from seawater on pH dynamics on the surface and inside the coelenteron of *G. fascicularis* polyps. pH dynamics on the surface (A) and inside the coelenteron (B) in normal seawater. pH dynamics on the surface (C) and inside the coelenteron (D) in Ci-free seawater. Dark bars indicate dark period and light bars indicate illumination.

The effect of CA inhibition on the concentration dynamics of Ca^{2+} inside the coelenteron is shown in Fig. 8. Inside the coelenteron, the dynamics has increased and the level of Ca^{2+} was higher in the inhibited (Fig. 8B) compared to the uninhibited polyps (Fig. 8A). Due to experimental problems, it was not possible to measure dynamics of calcium on the surface.

Dynamics of pH on the surface and inside the coelenteron were strongly affected by CA inhibition (Fig. 9). Upon EZ addition, surface pH decreased by ca. 0.6 units in light (from 8.74 to 8.15) (Fig. 9A&C). Inside the coelenteron, addition of EZ decreased pH by ca. 0.4 units in light (from 8.2 to 7.8) (Fig. 9B&C).

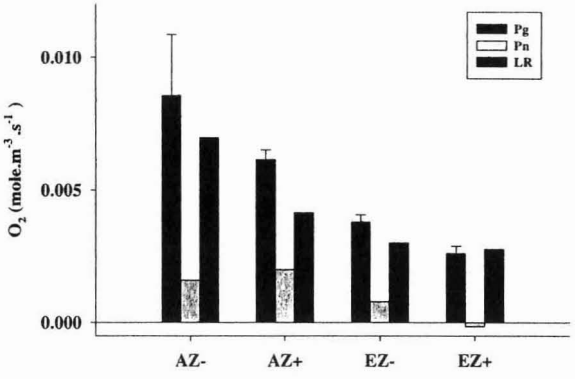

Fig. 7: Effect of Carbonic Anhydrase Inhibitors (AZ and EZ) on Pg, Pn and LR in *G. fascicularis* polyps. The –ve sign indicates the absence of inhibitor and the +ve sign indicates its presence.

4. Discussion:

4.1. Normal Physiology of the coral

The zooxanthellae within the coral tissue produce more O_2 than is needed by the animal, as the rate of gross photosynthesis (Pg) is more than the rate of light respiration (LR) (Fig. 2). CO_2 fixation and production of reduced organic compounds accompany the net O_2 production. Only 10-20% of the O_2 produced by the zooxanthellae is released to the surrounding environment, the rest is consumed.

Processes that reduce oxygen in light include oxidative phosphorylation, photorespiration and the Mehler reaction. In oxidative phosphorylation, the reduced organic compounds are oxidized to conserve ATP. In photorespiration, the ribulose bisphosphate is oxygenated rather than carboxylated by the enzyme Rubisco (Walker, 1992), while oxygen is reduced to superoxide by the reduced donors associated with photosystem I (PSI) in the Mehler reaction (Badger *et al.*, 2000). With microsensors technique we cannot determine the contributions of each pathway. However, photorespiration is not important in *Symbiodinium sp.* in the coral (Taylor and Trench, 1986), and the Mehler reaction is considered

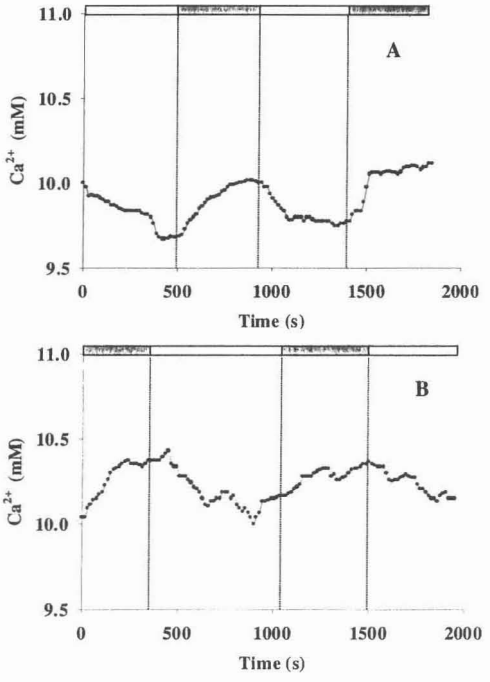

Fig. 8: Effect of EZ addition on Ca^{2+} dynamics inside the coelenteron. Ca^{2+} dynamics inside coelenteron (A) in normal seawater. Ca^{2+} dynamics inside the coelenteron after EZ addition (B). Dark bars indicate dark period and light bars indicate illumination.

insignificant in plants possessing C-3 carbon-fixation pathway (Badger *et al.*, 2000).

The C-3 carbon fixation characterizes *Symbiodinium sp.* (Streamer *et al.*, 1993). Therefore, we assume that the calculated oxygen consumption in light is mainly representing oxygen consumed in oxidative phosphorylation. In this case, Pg and LR form a highly active internal carbon cycle (C-cycle), whereby energy is produced that is used for many processes requiring energy in the polyp. Ca^{2+} dynamics to light/dark and dark/light switches on the surface and inside the coelenteron were similar, showing a decrease upon illumination and an increase upon darkening (Fig. 3). Thus, illumination increased the rate of Ca^{2+} uptake, while darkening decreased it. The concentration of Ca^{2+} is higher on the surface than inside the coelenteron and less than seawater in light. The Ca^{2+} concentration gradient is larger in the light than in the dark. This concentration gradient drives Ca^{2+} diffusion from seawater to

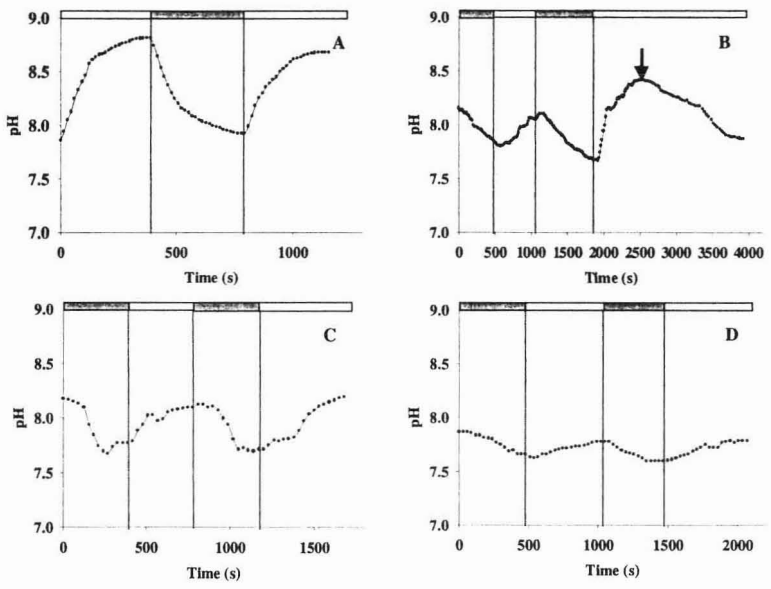

Fig. 9: Effect of EZ addition on pH dynamics on the surface and inside the coelenteron. pH dynamics on the surface without EZ (A) and inside the coelenteron before and after addition of EZ (B) (Arrow indicates addition of EZ). pH dynamics on the surface (C) and inside the coelenteron (D) with EZ. Dark bars indicate dark period and light bars indicate illumination.

the coelenteron, from which it is then further transported to the skeleton.

Photosynthesis and respiration affect surface pH through their uptake and release of CO_2. The pH increased in light and decreased in dark (Fig. 3). Inside the coelenteron, the pH also increased in light and decreased in dark. Compared to the pH dynamics on the surface, a lag period before an increase in pH was observed in response to light inside the coelenteron. This period is thought to be due to pumping of H^+ produced by calcification to the coelenteron (Al-Horani *et al.*, in preparation). And thus, alkalization caused by photosynthetic CO_2 uptake is balanced by this proton pumping. Because photosynthesis rate exceeds calcification rate in corals (Gattuso *et al.*, 1999), alkalization was observed after the described lag period. The comparatively large coelenteron space also affects the pH response to light/dark switches. The surface pH is more alkaline than inside the coelenteron in light

due to the protons pumped by calcification. The coelenteron is thus a passive compartment in between photosynthesis and the calcifying compartment, influenced by H^+ pumping from the calicoblastic layer, and photosynthesis induced pH shifts.

4.2. Details of the internal C-cycle

The difference between gross and net photosynthesis shows that photosynthesis can obtain most of its Ci from respiration. Indeed, in Ci-free seawater, Pg is only 14% lower than in normal seawater (Fig. 4). Thus photosynthetic CO_2 fixation can rely for some time on internal Ci sources. Rubisco performs both photosynthetic carbon reduction (PCR) and photorespiratory carbon oxidation (PCO), depending on the O_2/CO_2 ratios. High O_2/CO_2 ratios are known to enhance PCO (Laisk and Edwards, 1998). Respiration in the vicinity of the enzyme's active site may reduce PCO by reducing the O_2/CO_2 ratio. Thus this process is important for the intracellular functioning of Rubisco in PCR.

The total carbon (organic and inorganic) existing in the coral body (the tissue and the skeleton) represents an internal carbon pool (C-pool), and various processes add or take carbon from this pool. The organic carbon is added through plankton predation and consumption of suspended particulate matter (Ferrier-Pages *et al.*, 1998a; Anthony and Fabricius, 2000; Titlyanov *et al.*, 2000), while different mechanisms are used for Ci uptake from seawater. Withdrawal from the internal C-pool include the carbon used in biosynthesis, such as egg production and for building a new tissue (Rinkevich, 1991), synthesis of organic matrix (Allemand *et al.*, 1998b), mucus production (Ferrier-Pages *et al.*, 1998b; Schlichter and Brendelberger, 1998) and the Ci precipitated in the skeleton. We have conducted a study of the mechanisms involved in Ci uptake and use in photosynthesis and calcification.

The seawater contains 2.4 mM Ci, which in the present situation in the sea (pH is ca. 8.2), has > 99% of its Ci content in a non-permeable forms (HCO_3^- and CO_3^{2-}), while <1% present in a permeable form (CO_2). The use of permeable and impermeable CA inhibitors, EZ and AZ, respectively, demonstrated the presence of intracellular CA. Both inhibitors produced similar effect on Pg (ca. 30% inhibition), but had different effects on Pn and LR (Fig. 7). Thus, membrane bound and intracellular CA is present in the polyp and it helps exchanging the Ci between external and internal Ci-pools. In Fig. 6A&C and Fig. 9A&C, the surface pH has decreased in Ci-free seawater and upon inhibition of CA by EZ. This pH decrease might be due to pumping of protons to the surface by H^+-ATPase bound to the

membranes of the oral ectodermal cells facing the exterior, as it was also suggested in sea anemone, another member of class Anthozoa (Furla *et. al.*, 2000a). When CA is inhibited, this H^+ cannot efficiently react with HCO_3^-, thus instead lead to the observed pH decrease. Also, in Ci-free seawater the H^+ cannot react with HCO_3^- thus leads to pH decrease. These data indicate that membrane-bound CA uses the protons pumped to the surface by H^+-ATPase to convert the impermeable HCO_3^- and CO_3^{2-} to CO_2, which diffuses into cells and becomes available for photosynthesis. This localization of CA was also suggested in sea anemones (Benazet-Tambutte *et al.*, 1996) and corals (Furla *et al.*, 2000b). The pH responses to light/dark switches on the polyp surface (Fig. 3) indicated that, CO_2 is the major form of Ci transported from seawater to the cells rather than HCO_3^- or CO_3^{2-}. However, bicarbonate-carriers were also shown on the oral epithelium (Allemand *et al.*, 1998a; Furla *et al.*, 2000b). CA inhibition blocks CO_2 uptake by the coral as it was shown by de Beer *et al.*, (2000).

Ci is also obtained from seawater inside the coelenteron. Three factors influence the carbonate system of this compartment. These are (i) seawater-Ci influx through the mouth, (ii) Ci influx through the oral epithelium and (iii) protons produced by calcification pumped to the coelenteron. Acidification of the coelenteron upon exclusion of Ci from seawater (Fig. 6D) and upon CA inhibition (Fig. 9C&D) indicated that protons are pumped to the coelenteron. The pH decrease of 0.6 units in the coelenteron upon EZ addition indicated the presence of CA bound to the membranes of the endodermal cells facing the coelenteron (Fig. 9B). This CA is important for pH balance and controlling of the carbon speciation inside the coelenteron.

The Ci from metabolic respiration was shown to be incorporated into the $CaCO_3$ skeleton of the coral (Pears, 1970; Goreau, 1977). Pulse chase experiments with ^{14}C labeled glucose fed to *G. fascicularis* colonies were incorporated into the skeleton of the coral (unpublished data). For use of respiratory Ci, CO_2 might diffuse to the calcifying fluid (between the skeleton and the calicoblastic layer) and interact with H_2O to produce CO_3^{2-} according to the following series of reactions:

$$CO_2 + H_2O \Longleftrightarrow H_2CO_3 \Longleftrightarrow H^+ + HCO_3^- \Longleftrightarrow 2H^+ + CO_3^{2-}$$

In a previous study we showed that over the calicoblastic layer, protons are exchanged with Ca^{2+} by the enzyme Ca-ATPase. Thus, the pH of the calcifying fluid shifts the carbonate system toward CO_3^{2-} (Al-Horani *et al.*, in preparation).

There is a reversible exchange of Ca^{2+} between internal and external pools, as the skeleton seems to dissolve in Ci-free seawater. Thus, allocation of Ci from the skeleton to support photosynthesis is possible in corals. Under normal conditions this will not occur, but it underlines the notion that Ca^{2+} and Ci pools easily exchange.

Comparison of Ca^{2+} dynamics on the surface and inside the coelenteron in normal seawater and in Ci-free seawater showed that corals decalcify in the absence of external Ci (Fig. 5). The Ca^{2+} level in the two compartments was higher in Ci-free seawater than in normal seawater and higher than in the water column. The role of CA in calcification was also tested by addition of EZ. This inhibition increased Ca^{2+} level inside the coelenteron (Fig. 8). This increase in the level of Ca^{2+} upon CA inhibition indicated that less calcium is precipitated in the skeleton. Thus, the enzyme CA seems to be involved in the Ci use by calcification.

4.3. Conclusions

In scleractinian corals, there is a highly active internal C-cycle among photosynthesis and respiration. This cycle supplies ATP for the energy requiring processes in the animal. In this cycle, the organic carbon is consumed by respiration while the CO_2 produced by respiration is the main source of carbon fixed by photosynthesis. In this cycle, seawater-Ci and plankton consumed in the animal respiration are external sources of Ci supplied to photosynthesis and respiration, respectively. Ci for photosynthesis may also be allocated from the skeleton through the exchange process that the animal practices with the surrounding environment. Ci is supplied for calcification from the Ci of the C-cycle and from external seawater Ci.

Three CA localities were defined, the first is bound to the membranes of the ectodermal cells, the second is bound to the membranes of the endodermal cells facing the coelenteron and the third is intracellular. CA helps in the exchange of Ci for photosynthesis and calcification. It also helps pH balance inside the polyp.

The animal practices a dynamic exchange of calcium with the surrounding seawater.

Acknowledgements

This study has been funded by the German Federal Ministry of Education and Research (BMBF grants no. 03F0245A). We thank G. Eickert, A. Eggers and I. Schröder for constructing the oxygen electrodes, C. Stehning and G. Holst for technical support. We also thank the staff of the Marine Science Station in Aqaba-Jordan for supplying the diving equipments, Laboratory space and coral specimens.

Reference:

1. Allemand, D., Furla, P., Benazet-Tambutte, S., 1998a. Mechanisms of carbon acquisition for endosymbiont photosynthesis in Anthozoa. Can. J. Bot. 76, 925-941.

2. Allemand, D., Tambutte, E., Girard, J. P., Jaubert, J., 1998b. Organic matrix synthesis in the scleractinian coral Stylophora pistillata: Role in biomineralization and potential target of the organotin tributyltin. J. Exp. Biol. 201, 2001-2009.

3. Al-Moghrabi, S., Goiran, C., Allemand, D., Speziale, N., Jaubert, J., 1996. Inorganic carbon uptake for photosynthesis by the symbiotic coral-dinoflagellate association II. Mechanisms for bicarbonate uptake. J. Exp. Mar. Biol. Ecol. 199, 227-248.

4. Anthony, K. R. N., Fabricius, K. E., 2000. Shifting roles of heterotrophy and autotrophy in coral energetics under varying turbidity. J. Exp. Mar. Biol. Ecol. 252, 221-253.

5. Badger, M. R., Price, G. D., 1992. The CO_2 concentrating mechanism in cyanobacteria and microalgae. Physiol. Plant. 84,606-615.

6. Badger, M. R., von Caemmerer, S., Ruuska, S., Nakano, H., 2000. Electron flow to oxygen in higher plants and algae: rates and control of direct photoreduction (Mehler reaction) and rubisco oxygenase. Phil. T. R. S. Lond. B 355(1402), 1433-1445.

7. Barnes, D. J., Chalker, B. E., 1990. Calcification and photosynthesis in reef-building corals and algae. In Z. Dubinsky (ed.), Ecosystems of the world, coral reefs, 25, 109-131. Elsvier, Amsterdam.

8. Benazet-Tambutte, S., Allemand, D., Jaubert, J., 1996. Permeability of the oral epithelial layers in cnidarians. Mar. Biol. 126, 43-53.

9. De Beer, D., Kühl, M., Stambler, N., Vaki, L., 2000. A microsensor study of light enhanced Ca^{2+} uptake and photosynthesis in the reef-building hermatypic coral *Favia* sp. Mar. Ecol. Prog. Ser. 194, 75-85.

10. De Beer, D., Schramm, A., Santegoeds, C., Kühl, M., 1997. A nitrite microsensor for profiling environmental biofilms. App. Env. Microbiol. Mar. 63(3), 973-977.

11. Ferrier-Pages, C., Allemand, D., Gattuso, J. P., Jaubert, J., Rassoulzadegan, R., 1998a. Microheterotrophy in the zooxanthellate coral Stylophora pistillata: Effects of light and ciliate density. Limnol. Oceanogr. 43, 1639-1648.

12. Ferrier-Pages, C., Gattuso, J. P., Cauwet, G., Jaubert, J., Allemand, D., 1998b. Release of dissolved organic carbon and nitrogen by the zooxanthellate coral Galaxea fascicularis. Mar. Ecol.-Prog. Ser. 172, 265-274.

13. Furla, P., Allemand, D., Orsenigo, M. -N., 2000a. Involvement of H^+-ATPase and carbonic anhydrase in inorganic carbon uptake for endosymbiont photosynthesis. Am. J. Physiol. 278, R870-R881.

14. Furla, P., Galgani, I., Durand, I., Allemand, D., 2000b. Sources and mechanisms of inorganic carbon transport for coral calcification and photosynthesis. J. Exp. Biol. 203, 3445-3457.

15. Gattuso, J. -P., Allemand, D., Frankignoulle, M., 1999. Photosynthesis and calcification at cellular, organismal and community levels in coral reefs: a review on interaction and control by carbonate chemistry. Amer. Zool. 39,160-183.

16. Goiran, C., Al-Moghrabi, S., Allemand, D., Jaubert, J., 1996. Inorganic carbon uptake for photosynthesis by the symbiotic coral/dinoflagellate association I. Photosynthetic performances of symbionts and dependence on sea water bicarbonate. J. Exp. Mar. Biol. Ecol. 199, 207-225.

17. Goreau, T. J., 1977. Coral skeletal chemistry: physiological and environmental regulation of stable isotopes and trace metals in *Montastrea annularis*. Proc. R. Soc. Lond. B. 196, 291-315.

18. Hochachka, P. W., Somero, G. N., 1973. Strategies of biochemical adaptation. E. B. Saunders Company. Philadelphia.

19. Jordan, D. B., Ogren, W. L., 1981. Species variation in the specificity of ribulose bisphosphate carboxylase/oxygenase. Nature. 291, 513-515.

20. Kingsley, R. J., Watabe, N., 1987. Role of carbonic anhydrase in calcification in the gorgonian *Leptogorgia virgulata*. J. Exp. Zool. 241, 171-180.

21. Kühl, M., Cohen, Y., Dalsgaard, T., Jorgensen, B. B., Revsbech, N. P., 1995. Microenvironment and photosynthesis of zooxanthellae in scleractinian corals studied with microsensors for O_2, pH and light. Mar. Ecol. Prog. Ser. 117, 159-172.

22. Laggat, W., Rees, T. A. V., Yellowlees, D., 2000. Meeting the photosynthetic demand for inorganic carbon in an alga-invertebrate association: preferential use of CO_2 by symbionts in the giant clam *Tridacna gigas*. Proc. Royal Soc. London-Biol. Sci. 267, 523-529.

23. Laisk, A., Edwards, G. E., 1998. Oxygen and electron flow in C-4 photosynthesis: Mehler reaction, photorespiration and CO_2 concentration in the bundle sheath. PLANTA 205(4), 632-645.

24. Marubini, F., Thake, B., 1999. Bicarbonate addition promotes coral growth. Limnol. And Oceanogr. 44(3), 716-720.

25. Pears, V. B., 1970. Incorporation of metabolic CO_2 into coral skeleton. Nature. 228, 383

26. Revsbech, N. P., Jorgensen, B. B., 1983. Photosynthesis of benthic microflora measured with high spatial resolution by the oxygen microprofile method. Limnol. Oceanogr. 28(4), 749-756.

27. Rinkevich, B., 1991. A long-term Compartmental Partitioning of Photosynthetically Fixed Carbon in a Symbiotic Reef Coral. Symbiosis. 10, 175-193.

28. Schlichter, D., Brendelberger, H., 1998. Plasticity of the scleractinian body plan: Functional morphology and trophic specialization of *Mycedium elephantotus* (Pallas, 1766). Facies. 39, 227-241.

29. Sekino, K. and Shiraiwa, Y., 1994. Accumulation and utilization of dissolved inorganic carbon by a marine unicellular coccolithophorid, *Emiliania huxleyi*. Plant Cell Physiol. 35, 353-361.

30. Smith, S. V., 1978. Coral reef area and the contributions of reefs to processes and resources of the world's oceans. Nature. 273, 225-226.

31. Streamer, M., McNeil, Y. R., Yellowlees, D., 1993. Photosynthetic carbon dioxide fixation in zooxanthellae. Mar. Biol. 115(2), pp. 195-198.

32. Taylor, E. M., Trench, R. K., 1986. Activities of enzymes in β-carboxylation reactions and of catalase in cell-free preparations from the symbiotic dinoflagellates Symbiodinium spp. from a coral, a clam, a zoanthid and two sea anemones. Proc. R. Soc. Lond. B 228, 483-492.

33. Titlyanov, E. A., Leletkin, V. A., Dubinsky, Z., 2000. Autotrophy and predation in the hermatypic coral Stylophora pistillata in different light habitats. Symbiosis. 29, 263-281.

34. Walker, D., 1992. Excited leaves. New Phytol. 121, 325-345.

Chapter 3

Mechanism of calcification and its relation to photosynthesis and respiration in the scleractinian coral *Galaxea fascicularis*

Manuscript submitted for publication in Marine Biology

Mechanism of calcification and its relation to photosynthesis and respiration in the scleractinian coral *Galaxea fascicularis*

Fuad A. Al-Horani[1, 2], Salim M. Al-Moghrabi[2], Dirk de Beer[1]
1. Max Planck Institute for Marine Microbiology, Celsiusstrasse 1, D-28359 Bremen, Germany
2. Marine Science Station, P. O. Box (195), Aqaba, 77110 Jordan

Abstract

The mechanism of calcification and its relation to photosynthesis and respiration in the scleractinian coral, *Galaxea fascicularis* was studied with microsensors for Ca^{2+}, pH and O_2. Gross photosynthesis (Pg), net photosynthesis (Pn) and dark respiration (DR) and light respiration (LR) was calculated from the difference between Pg and Pn. Pg was ca. 7 times higher than Pn, thus respiration consumes most of the O_2 produced by the symbiont photosynthesis. The coupled Pg and LR thus cause an intensive internal carbon and O_2 cycling. The resultant of this cycle is metabolic energy (ATP). The measured ATP content was 35% higher in light incubated colonies than in dark incubated ones. The respiration rate in light was ca. 12 times higher than in the dark.

Direct measurements of Ca^{2+} and pH dynamics were done on the surface, inside the polyp's coelenteron and under the calicoblastic layer. The effects of light/dark and dark/light switches on Ca^{2+} and pH dynamics were followed in the three compartments. Ca^{2+} concentrations decreased in light on the surface and in the coelenteron compartments and increased upon switching light off. Under the calicoblastic layer the opposite was observed. In light, the level of Ca^{2+} was lower on the surface than in seawater, and even lower inside the coelenteron. Under the calicoblastic layer, the concentration of calcium was ca. 0.5-1 mM higher than seawater. Thus Ca^{2+} can diffuse from seawater to the coelenteron, but metabolic energy is needed for the transport across the calicoblastic layer to the skeleton. The pH under the calicoblastic layer was alkaline compared to the surface and inside the coelenteron. Because of this, the aragonite saturation state under the calicoblastic layer has increased from ca. 3.2 in the dark to ca. 25 in the light, creating an excellent environment for calcification at high rate in light.

When Ruthenium Red (specific inhibitor of Ca-ATPase) was added, Ca^{2+} and pH dynamics were inhibited under the calicoblastic layer. This indicated that Ca-ATPase transports Ca^{2+} against its gradient in exchange for H^+ at the calicoblastic layer. Addition of DCMU (PSII inhibitor) completely inhibited photosynthesis. The calcium dynamics under the calicoblastic layer continued, however, they were less regular. The initial rates were maintained. We concluded that light and not energy generation triggers calcium uptake, however energy (mainly supplied from respiration of photosynthates) is also needed.

Keywords: coral, *Galaxea fascicularis*, calcification, photosynthesis, dark respiration, light respiration, C-cycle, Ca-ATPase, carbonic anhydrase, calicoblastic layer, microsensors.

Introduction

Scleractinian corals are abundant in oligotrophic environments (tropical seas). This success was attributed to their association with symbiotic dinoflagellates called *Symbiodinium sp.* (commonly known as zooxanthellae). Corals precipitate aragonite $CaCO_3$ to produce supportive skeletons (Barnes 1970). It is well documented that light enhances calcification (e.g. Goreau, 1959, Pears & Muscatine, 1971). The mechanism of this enhancement though is still debated (Marshal, 1996; Carlon, 1996; Goreau et al. 1996). The lack of understanding limits predictions of future changes in the rate of calcification in response to global climate change (Gattuso et al. 1999). Also the interactions of calcification with endosymbiont photosynthesis are poorly known (Gattuso, et al. 2000). The conflicting theories proposed include that (i) energy supply by zooxanthellae is responsible for light enhanced calcification (Goreau, 1959; Chalker & Taylor, 1975), (ii) calcification generates protons used to assimilate bicarbonate and nutrients (McConnaughey & Whelan, 1997), (iii) both processes are more efficient in the coexisting system than in the isolated reactions (Suzuki et al. 1995) and that (iv) calcification does not enhance photosynthesis (Yamashiro, H., 1995; Gattuso, et al. 2000). Two forms of Ca-ATPases were characterized that may play a role in calcification (Kingsley & Watabe, 1985; Ip et al. 1991) however the exact mechanism of this role was not yet revealed.

Corals form a multi-compartment structure composed of two epithelial layers (oral and aboral) separated by the coelenteron. The calcifying layer (calicoblastic layer) faces the skeleton, while the symbionts (zooxanthellae) are present within a perisymbiotic membrane in

the endodermal cells. Due to the close structural arrangement, the processes involved have not been measured directly so far. Microsensors enabled us to measure with high spatial and temporal resolution of biological processes occurring in different localities and compartments of the coral polyp.

Oxygen microsensors have been used to measure gross (Pg) and net (Pn) photosynthesis rates and dark respiration (DR), as well as Ca^{2+} and pH dynamics on the surface of the corals; *Favia* and *Acropora* (Kühl et al. 1995; De Beer et al. 2000). In this study, we measured with microsensors in deeper layers of the coral *G. fascicularis* polyp and the calcification site. Specific inhibitors for Ca-ATPase, PSII and carbonic anhydrase (CA) were also used.

Materials and Methods

Biological samples

Galaxea fascicularis colonies were collected by SCUBA diving from 5-m depth south of the Marine Science Station, Aqaba-Jordan. The collected colonies were immediately transferred to a $2m^3$ aquarium with seawater and illuminated with HQI-lamp with a light spectrum and intensity similar to the natural light (12hr: 12hr light-dark cycle). The colonies were fragmented into smaller microcolonies and left for at least two weeks to acclimatize to the aquarium conditions before use.

Inhibitors

The specific inhibitor of PSII, dichlorophenyldimethylurea (DCMU) was dissolved in ethanol and added to a final concentration of 1 μM. Ruthenium red (RR) (a specific inhibitor of Ca-ATPase) was dissolved in dimethylsulfoxide (DMSO) and added to a final concentration of 100 μM. Acetazolamide (AZ), the specific inhibitor of carbonic anhydrase was dissolved in DMSO and added to a final concentration of 600 μM. The final concentration of DMSO and ethanol was 0.1%.

Microsensors

Ca^{2+} microsensors (de Beer et al. 2000), Clark type O_2 electrodes (Revsbech and Jorgensen, 1983) and LIX pH electrodes (de Beer et al. 1997) were constructed and calibrated as described and positioned on the polyp surface, inside the coelenteron and under the calicoblastic layer. Pg rate was measured using the light dark shift method as described in (Kühl et al. 1995). O_2 profiles in light and dark were used to calculate Pn and DR rate using Fick`s first low of diffusion, assuming 100 μm photosynthetically active tissue thickness. LR was calculated from the difference between Pg and Pn.

Experimental set-up

Coral colonies were placed in a polycarbonate flow cell with a volume of 0.7 L for microsensor measurements. Filtered seawater was circulated between the flow cell and a 3 L reservoir at a constant flow rate (420 ml/min). The water had 4% salinity, pH 8.2-8.3 and ambient temperature of 20-21°C. The reservoir was continuously aerated. Motorized micromanipulators fixed on a heavy stand were used to position the electrodes. A halogen light source (KL 1500 Schott Mainz company-Germany) provided a light intensity of 140-μmole photons m^{-2} s^{-1}. A shutter (Uniblitz Electronic) controlled the light entrance. Signals from the millivoltmeter and the picoamperometer were plotted on a strip-chart recorder.

Positioning of the microsensors

Positioning of the electrodes on the surface of *G. fascicularis* polyps was done as described previously (de Beer et al. 2000). The coelenteron was accessed through the mouth. The sensors were brought at the calcifying site by making an incision with a scalpel, lifting the tissue gently from the skeleton by a water jet and then positioning the sensors under the calicoblastic layer. Because this might disturb the chemical conditions of the microenvironment under the calicoblastic layer, the tissue was left for at least one hour to relax and cover the microsensor and give enough time to re-establish normal condition before measurements were taken.

ATP determination

Microcolonies of *G. fascicularis* were incubated in light (140 μmole photons m^{-2} s^{-1}) and dark in normal seawater (aerated and circulated at 26°C for 3 hrs each). The incubated microcolonies were transferred to 1 M NaOH and 50 mM Na-EDTA solution and heated at 90°C for 15 minutes. The hydrolysate was centrifuged at 4500 rpm for 30 minutes. The pH of the supernatant was adjusted to ca. 7.8. The ATP content was determined following a luminometric method described in Promega kit (Promega co. USA). Protein content was analyzed by the Bradford method (1976).

Calculation of the saturation state

The aragonite saturation state was calculated (using the Solmineq.88 software assuming a dissolved inorganic carbon concentration of 2.4 mM, temperature of 21°C and 4% salinity).

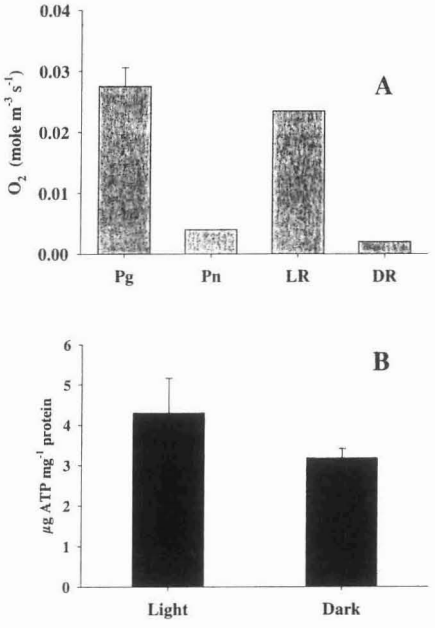

Fig. 1: Rates of gross (Pg) and net (Pn) photosynthesis, and light (LR) and dark (DR) respiration (A). ATP concentration in light and dark incubated colonies (B).

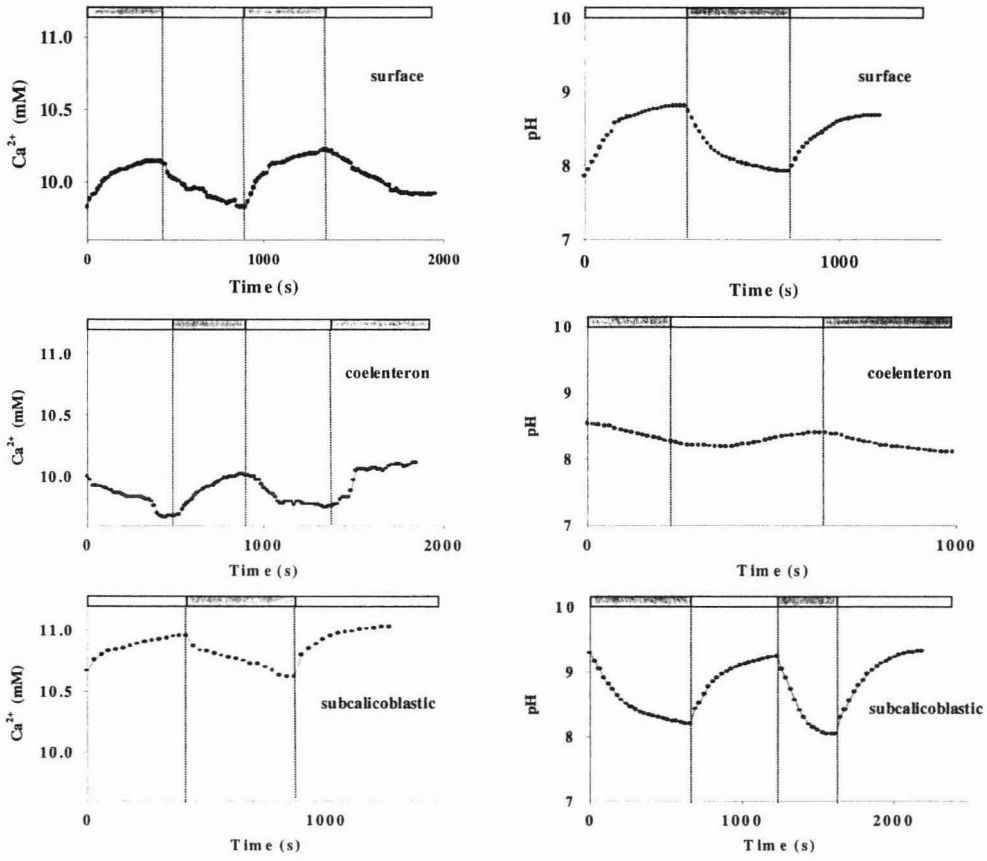

Fig. 2: Dynamics of Ca^{2+} and pH on the surface, inside the coelenteron and under the calicoblastic layer in *G. fascicularis*. Dark bars indicate dark period and light bars indicate illumination.

Results

Photosynthesis, respiration and energy budget

The rate of gross photosynthesis (Pg) was ca. 7 times higher than the rate of net photosynthesis (Pn). Thus the light respiration (LR) was ca. 80-90% of Pg. The LR was ca. 12 times higher than the respiration rate in the dark (DR) (Fig. 1A). The measured ATP concentration in microcolonies incubated in light was ca. 35% higher than those incubated in

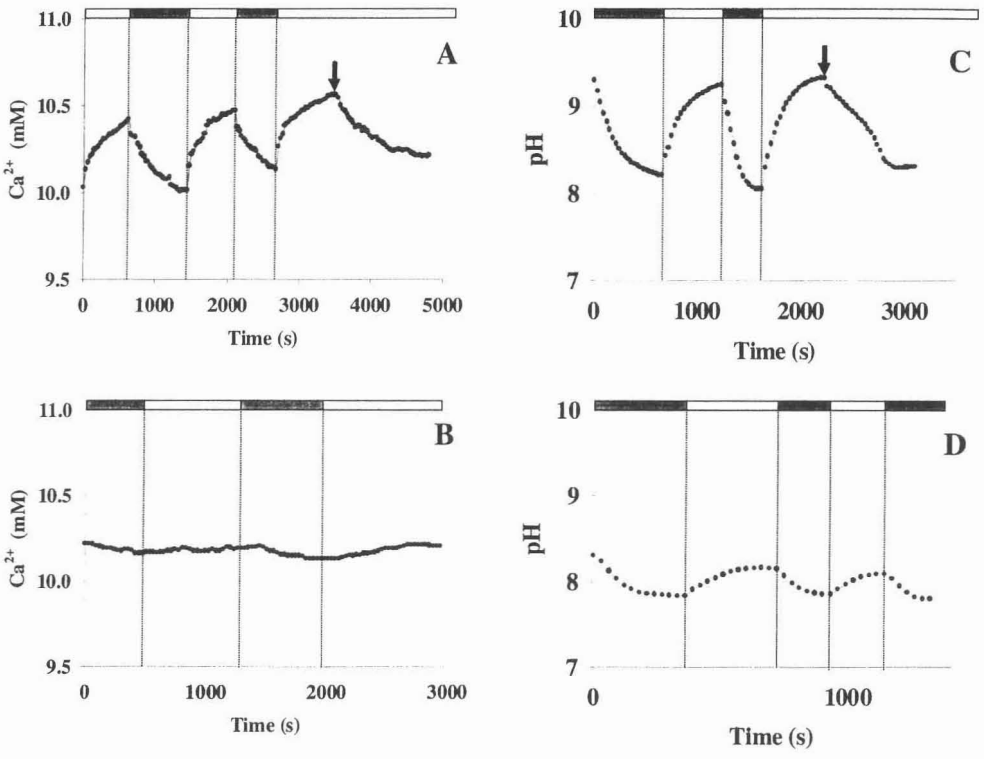

Fig. 3: Effects of illumination on Ca^{2+} (A & B) and pH (C & D) dynamics under the calicoblastic layer before and after addition of Ruthenium Red (RR). Arrows indicate addition of RR inhibitor. Dark bars indicate dark period and light bars indicate illumination.

dark (illuminated samples: 4.3 ± 0.87 (n=9) μg ATP mg^{-1} protein; dark incubated samples: 3.17 ± 0.23 (n=9) μg ATP mg^{-1} protein) (Fig.1B).

Calcium and pH dynamics

The effects of light/dark and dark/light switches on Ca^{2+} and pH dynamics were measured on the surface, inside the coelenteron and under the calicoblastic layer. Switching the light on decreased Ca^{2+} concentration on the surface and inside the coelenteron and increased it

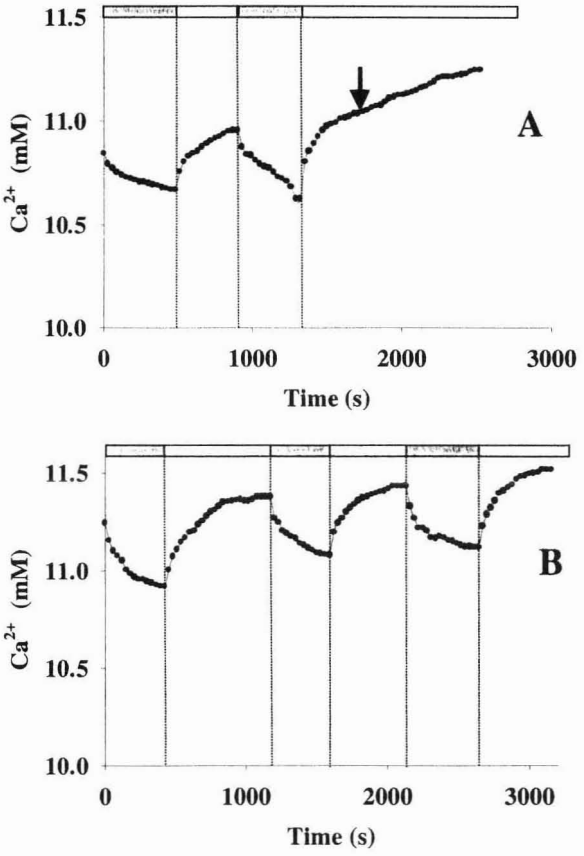

Fig. 4: Effect of carbonic anhydrase inhibition on the dynamics of Ca^{2+} under the calicoblastic layer. The arrow indicates addition of Acetazolamide inhibitor (AZ). Dark bars indicate dark period and light bars indicate illumination. (A) Dynamics before and upon addition of AZ. (B) Dynamics after addition of AZ.

under the calicoblastic layer, while switching the light off reversed the situation. Switching the light on increased the pH and switching to dark decreased it in the three compartments. The Ca^{2+} dynamics on the polyp surface and inside the coelenteron were opposite to the dynamics under the calicoblastic layer (Fig. 2). In light, the concentration of Ca^{2+} on the surface (ca. 9.8 mM) was higher than the concentration inside the coelenteron (ca. 9.6 mM) and less than the

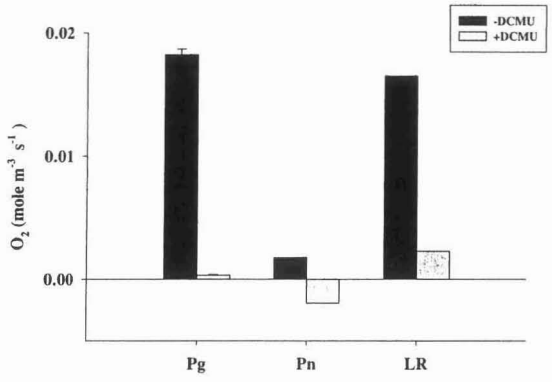

Fig. 5: Effect of DCMU addition on the rates of gross photosynthesis (Pg), net photosynthesis (Pn) and light respiration (LR) in the coral *G. fascicularis*.

concentration in seawater (10.0 mM). Under the calicoblastic layer, the level of calcium was ca. 1-1.5 mM higher than inside the coelenteron in light and the pH was ca. 9.3 (Fig. 2). The calculated aragonite saturation state was ca. 25 in light compared to ca. 3.2 in dark and ca. 4 in seawater.

Effect of inhibitors

Addition of Ca-ATPase inhibitor (RR) inhibited Ca^{2+} and pH dynamics under the calicoblastic layer in light to dark level (Fig. 3). Inhibition of carbonic anhydrase (CA) by AZ increased the concentration dynamics of calcium under the calicoblastic layer (Fig. 4). DCMU completely inhibited Pg (Fig. 5) and decreased the amplitude of the Ca^{2+} concentration dynamics under the calicoblastic layer with ca. 50% (Fig. 6). The dynamics after inhibition were less regular. The initial Ca^{2+} concentration increase under the calicoblastic layer observed upon switching on the light was not affected by DCMU.

Discussion and conclusions

Energy budget

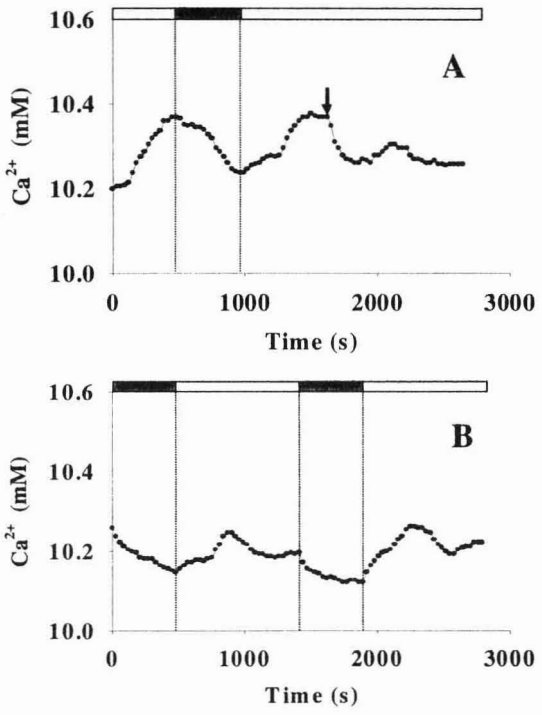

Fig. 6: Effect of illumination and DCMU addition on Ca^{2+} dynamics under the calicoblastic layer. Arrow indicates addition of DCMU. Dark bars indicate dark period and light bars indicate illumination. (A) Dynamics before and upon addition of DCMU. (B) Dynamics after addition of DCMU.

In the untreated experiments (regular conditions), the rate of oxygen production (gross photosynthesis) by the symbiont exceeds the rate of its consumption (respiration); thus O_2 is released to the environment (net photosynthesis is positive value). Light respiration is the sum of at least three different processes: (1) photorespiration in which ribulose bisphosphate is oxygenated by the enzyme Rubisco and produce phosphoglycolic acid (Marx 1973), (2) the Mehler reaction in which oxygen is reduced to superoxide by the reduced donors associated with photosystem I (PSI) (Walker 1992) and (3) oxidative phosphorylation by mitochondria. The amount of oxygen reduced by photorespiration and the Mehler reaction is considered insignificant in the zooxanthellae when present in hospite (Taylor and Trench 1986; Badger et

al. 2000). Thus, oxidative phosphorylation by mitochondria is the major process that consumes oxygen produced by photosynthesis in the light. Only oxidative phosphorylation generates ATP. ATP is not generated by photorespiration (Wingler et al. 2000) and the Mehler reaction.

Metabolic respiration by the animal and the symbiont and photosynthesis by the symbiont form a highly active internal carbon cycle in the coral. The main function of this carbon cycle is the production of ATP to support energy requiring processes in the animal. Respiration rate in light (LR) is much higher than its rate in dark and thus more ATP is generated by the polyp in light than in dark. This is supported by the finding that the amount of ATP extracted from colonies incubated in light was ca. 35% higher than dark incubated colonies. Such increase in the ATP concentration in the light lead to an increase in the rate of the ATP-consuming processes (Raven, 1976) such as calcification process. Although, the LR/DR ratio is ca. 12, the amount of ATP extracted from colonies incubated in light is only 35% higher than those incubated in dark. Most likely, ATP is consumed at a faster rate in light than in the dark, thus the size of the ATP pool does not reflect proportionally the ATP production rate.

The use of metabolic inhibitors such as sodium cyanide and iodoacetic acid showed that energy is required for calcification to proceed (e.g. Chalker and Taylor 1975; Tambutte et al. 1996; Lucas and Knapp, 1997). Energy is needed in calcification for the transport of ions and synthesis of organic matrix (Chalker and Taylor, 1975). The organic matrix might include glycoproteins, proteins and phospholipids and function in nucleation and controls crystal growth (Young et al. 1971; Mitterer 1978; Constantz and weiner, 1988; Isa and Okazaki, 1987; Allemand et al. 1998). The synthesis and translocation of such organic matrix was suggested to be a prerequisite for calcification (Allemand et al. 1998). The main source of organic carbon respired comes from photosynthesis by the zooxanthellae (McCloskey and Muscatine, 1984; Porter et al. 1984). Various forms of carbohydrates are synthesized by the symbiont (Streamer et al. 1993) that are transported to growing parts of the polyp to generate ATP (Pears and Muscatine 1971; Fang et al. 1989). Cyclic photophosphorylation, another light dependent process, supplies ATP needed for synthesis of proteins and lipids that might be used by calcification (Furbank and Horton, 1987; Herzig and Dubinsky, 1993). The ATP molecules per

se, produced by cyclic photophosphorylation could not be supplied for the animal calcification as it is produced in the zooxanthellae and the membranes are not permeable for ATP.

Calcification mechanism

The concentration dynamics of calcium in light showed that the animal transports Ca^{2+} from seawater to the skeleton site by passive and active transport mechanisms (Fig. 2). Comparison of Ca^{2+} concentrations in seawater, on the surface and inside the coelenteron shows a downward gradient of Ca^{2+} between seawater and the coelenteron. This concentration gradient drive Ca^{2+} diffusion from seawater to the coelenteron as it was also demonstrated by Benazet-Tambutte et al. (1996). Under the calicoblastic layer, the level of Ca^{2+} is ca. 1.0-1.5 mM above its level inside the coelenteron in light. Thus, active transport of Ca^{2+} must take place for the transport of the ion against its concentration gradient across the calicoblastic layer to the skeleton site. The use of Ruthenium Red (a specific inhibitor of Ca-ATPase) stopped the dynamics of Ca^{2+} and pH under the calicoblastic layer (Fig. 3). Thus the Ca-ATPase transports Ca^{2+} to the skeleton site in exchange for H^+, thereby increasing the saturation states of Ca^{2+} and CO_3^{2-}. The aragonite saturation state under the calicoblastic layer increased from ca. 3.2 in dark to ca. 25 in light compared to ca. 4 in seawater. This change in the aragonite saturation state drives calcification at the skeleton. When such environment was mimicked by increasing the pH of filtered seawater to a value of 9.3, $CaCO_3$ immediately precipitated. The changes in Ca^{2+} and pH were fast indicating high activity of the enzyme Ca-ATPase. This high activity of Ca-ATPase is important for keeping very low intracellular Ca^{2+} level (Barnes and Chalker, 1990). The ATP needed for functioning of Ca-ATPase could be supplied from respiration as indicated from the higher rate of LR compared to DR.

Upon switching the light off, Ca^{2+} leak out was observed for a short period of time (Fig. 2). Such leak out of the ion might be due to a change in the pH at the skeleton site, which could release Ca^{2+} from the phospholipids in the organic matrix (Isa and Okazaki 1987). It is unknown how exactly Ca^{2+} is leaking through the calicoblastic layer and further research is needed.

The pH in the three compartments increased in light and decreased in dark (Fig. 2). Under the calicoblastic layer, the pH was more alkaline compared to pH on the surface and inside the coelenteron in light. Here, the pH reached ca. 9.3 in light and decreased to ca. 8.1 in

dark. At these pH values, the concentration of CO_3^{2-} is 7x higher in light than in dark and is the dominant form of inorganic carbon under the calicoblastic layer in light (pKa = 9.18 in seawater at 20°C (Stumm and Morgan, 1996)).

Pumping of protons from the subcalicoblastic layer to the coelenteron by Ca^{2+}-H^+-ATPase could decrease the pH inside the coelenteron, but this was not observed (Fig. 2). The decrease in pH by proton pumping as a result of calcification is opposed by the photosynthetic CO_2 uptake by the symbiont in the adjacent endodermal cells. Thus, the expected decrease in the coelenteron pH can't be seen as it is influenced by more than one process.

The role of CA in calcification was tested through the use of AZ. This CA inhibition caused an increase in Ca^{2+} concentration under the calicoblastic layer (Fig. 4). Probably this is due to a decreased calcification rate caused by the decrease in supply of carbonate ions at the skeleton site. This result agrees with results obtained by Furla et al. (2000) where calcification decreased by CA inhibition. Thus CA in the calcifying zone facilitate uptake of inorganic carbon for calcification, as it is Ci-limited (Marubini and Thake, 1999). The enzyme might also function in regulating the local pH by using protons generated by calcification in the conversion of bicarbonate to CO_2.

Addition of 1 μM of DCMU stopped oxygenic photosynthesis instantly (Fig. 5), however, the light-dependant calcium dynamics continued, although at lower amplitude (ca. 50%) (Fig. 6). The dynamics were smaller and showed some irregularity, i.e. the instant increase after illumination was followed by a decrease. The data are consistent with the hypothesis that the calcium transport to the skeleton site is directly triggered by light and not by energy generation. However, energy is needed and ATP is constantly re-supplied mainly from photosynthesis driven respiration.

Working model

We have integrated our results with those from literature in a model to explain the mechanism of calcification in corals (Fig. 7). In this model, Ca-ATPase generates two gradients of Ca^{2+} by continuously pumping Ca^{2+} to the calcifying site in light, and thus decreases the concentration of calcium in the calicoblastic cells and the coelenteron, at the same time it

	pH	Ca^{2+} (mM)	Aragonite saturation state
Seawater	**8.2**	**10.0**	**4.0**
Polyp Surface	**8.8**	**ca. 9.8**	
Coelenteron	**8.5**	**ca. 9.6**	
Calcifying Fluid	**9.3 (light)** **8.2 (dark)**	**10.5-11.0 (light)** **10.2-10.4 (dark)**	**25.0 (light)** **3.2 (dark)**

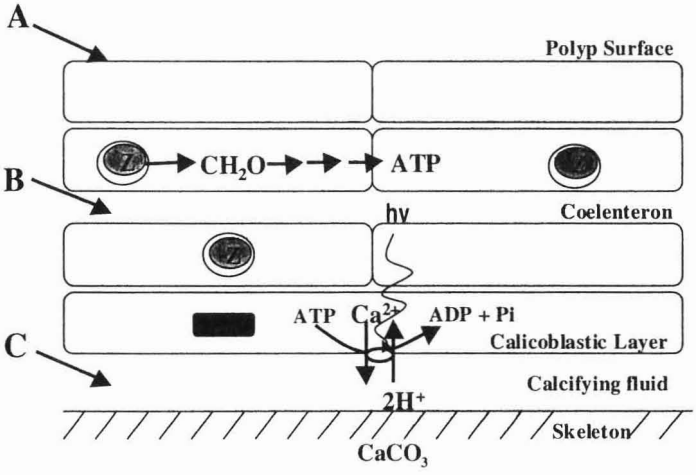

Fig. 7: Top: summary table of the data for calcium and pH values obtained in the three compartments illustrated in the drawing and the calculated aragonite saturation sate in seawater and in the calcifying fluid in light and dark conditions. Bottom: a conceptual model to explain the mechanism of light enhanced calcification in *G. fascicularis* illustrated on a simplified cross section of the coral. Ca-ATPase is present at the calicoblastic cells and pumps Ca^{2+} against concentration gradient in exchange for protons thereby increasing the saturation states of Ca^{2+} and CO_3^{2-} and thus $CaCO_3$ precipitates. ATP is supplied mainly from respiration of photosynthates. Z: zooxanthellae, Mt: mitochondria.

increases calcium concentration at the calcifying site. This leads to continuous diffusion of Ca^{2+} to the calicoblastic cells along the concentration gradient from seawater. The aragonite saturation state is increased strongly, from ca. 3.2 in the dark to ca. 25 in the light at the calcifying site. The transport of Ca^{2+} to the calcifying site is coupled to transport of protons away from it and the pH is increased to ca. 9.3, thereby increasing the carbonate concentration at the calcification site. These conditions favor high rates of calcification in light compared to dark. Oxidative phosphorylation of photosynthates and cyclic photophosphorylation by PSI supply the ATP needed to power ATP requiring processes in light.

Acknowledgments

This study has been funded by the German Federal Ministry of Education and Research (BMBF grants no. 03F0245A). We thank G. Eickert, A. Eggers and I. Schröder for constructing the oxygen electrodes, T. Ferdelman, M. Böttcher, C. Stehning, G. Holst and P. Stief for technical support. We also thank the staff of the Marine Science Station in Aqaba-Jordan for supplying the diving equipments, Laboratory space and coral specimens.

References

1. Allemand D, Tambutte E, Girard JP, Jaubert J (1998) Organic matrix synthesis in the scleractinian coral *Stylophora pistillata*: role in biomineralization and potential target of the organotin tributyltin. J Exp Biol 201: 2001-2009.

2. Badger MR, von Caemmerer S, Ruuska S, Nakano H (2000) Electron flow to oxygen in higher plants and algae: rates and control of direct photoreduction (Mehler reaction) and rubisco oxygenase. Phil. T R S Lond B 355(1402): 1433-1445.

3. Barnes DJ (1970) Coral skeletons: an explanation of their growth and structure. Science 170: 1305-1308.

4. Barnes DJ Chalker BE (1990) Calcification and photosynthesis in reef-building corals and algae. In Z. Dubinsky (ed.), Ecosystems of the world, coral reefs, vol.25, pp. 109-131. Elsvier, Amsterdam.

5. Benazet-Tambutte S, Allemand D, Jaubert J (1996) Permeability of the oral epithelial layers in cnidarians. Mar Biol 126: 43-53.

6. Carlon DB (1996) Calcification rates in corals. Science 271: 117.

7. Chalker BE, Taylor DL (1975) Light-enhanced calcification, and the role of oxidative phosphorylation in calcification of the coral *Acropora cervicornis*. Proc R Soc Lond B 190: 323-331.

8. Constantz B, weiner S (1988) Acidic macromolecules associated with mineral phase of scleractinian coral skeletons. J Exp Zool 248: 253-258.

9. De Beer D, Kühl M, Stambler N, Vaki L (2000) A microsensor study of light enhanced Ca^{2+} uptake and photosynthesis in the reef-building hermatypic coral *Favia* sp. Mar Ecol Prog Ser 194: 75-85.

10. De Beer D, Schramm A, Santegoeds C, Kühl M (1997) A nitrite microsensor for profiling environmental biofilms. App Env Microbiol Mar 63: 973-977.

11. Erez J (1978) Vital effect on stable-isotope composition seen in foraminifera and coral skeletons. Nature 273: 199-202.

12. Erez J (1983) Calcification rates, photosynthesis and light in planktonic foraminifera. In: P. Westbroek and E. W. de Jong (eds.), Biomineralization and Biological Metal Accumulation. Pp. 307-312, by D. reidel Publishing Company.

13. Fang LS, Chen YWJ, Chen CS (1989) Why does the white tip of stony coral grow so fast without zooxanthellae? Mar Biol 103: 359-363.

14. Furbank RT, Horton P (1987) Regulation of photosynthesis in isolated barely protoplast: the contribution of cyclic photophosphorylation. Biochemica et Biophysica Acta. 894: 332-338.

15. Furla P, Galgani I, Durand I, Allemand D (2000) Sources and mechanisms of inorganic carbon transport for coral calcification and photosynthesis. J Exp Biol 203: 3445-3457.

16. Gattuso JP, Allemand D, Frankignoulle M (1999) Photosynthesis and calcification at cellular, organismal and community levels in coral reefs: a review on interaction and control by carbonate chemistry. Am Zool 39: 160-183.

17. Gattuso JP, Reynaud-Vaganay S, Furla P, Romaine-Lioud S, Jaubert J, Bourge I, Frankignoulle M (2000) Calcification does not stimulate photosynthesis in the zooxanthellate scleractinian coral *Stylophoran pistillata*. Limnol Oceanogr 45: 246-250.

18. Goreau TF (1959) The physiology of skeleton formation in corals. I. A method for measuring the rate of calcium deposition by corals under different conditions. Biol Bull 116: 59-75.

19. Goreau TF (1963) Calcium carbonate deposition by coralline algae and corals in relation to their roles as reef-builders. Ann NY Acad Sci 109: 127-167.

20. Goreau TJ, Goreau NI, Trench RK, Hayes RL (1996) Calcification rates in corals. Science 271: 117.

21. Herzig R, Dubinsky Z (1993) Effect of photoacclimation on the energy partitioning between cyclic and non-cyclic photophosphorylation. New Phytol 123: 665-672.

22. Ip YK, Lim ALL, Lim RWL (1991) Some properties of calcium-activated adenosine triphosphatase from the hermatypic coral *Galaxea fascicularis*. Mar Biol 111: 191-197.

23. Isa Y, Okazaki M (1987) Some observations on the calcium binding phospholipid from scleractinian coral skeletons. Comp Biochem Physiol 87B: 507-512.

24. Kingsley RJ, Watabe N (1985) Ca-ATPase localization and inhibition in the gorgonian *Leptogorgia virgulata* (Lamarck) (Coelentrata: Gorgonacea). J Exp Mar Biol Ecol 93: 157-167.

25. Kühl M, Cohen Y, Dalsgaard T, Jorgensen BB, Revsbech NP (1995) Microenvironment and photosynthesis of zooxanthellae in scleractinian corals studied with microsensors for O_2, pH and light. Mar Ecol Prog Ser 117: 159-172.

26. Lucas JM, Knapp LW (1997) A physiological evaluation of carbon sources for calcification in the octocoral *Leptogorgia virgulata* (Lamarck). J Exp Biol 200: 2653-2662.

27. Marubini F, Thake B (1999) Bicarbonate addition promotes coral growth. Limnol. Oceanogr 44: 716-720.

28. Marx JL (1973) Photorespiration: key to increasing plant productivity? Science 179: 365-367.

29. McCloskey LR, Muscatine L (1984) Production and respiration in the Red Sea coral Stylophora pistillata as a function of depth. Proc R Soc Lond B 222: 215-230.

30. McConnaughey TA, Whelan JF (1997) Calcification generates protons for nutrient and bicarbonate uptake. Earth Science reviews 42: 95-117.

31. Mitterer RM (1978) Amino acid composition and metal binding capability of the skeletal protein of corals. Bull Mar Sci 28: 173-180.

32. Pears VB, Muscatine L (1971) Role of symbiotic algae (zooxanthellae) in coral calcification. Biol Bull 141: 350-363.

33. Porter JW, Muscatine L, Dubinsky Z, Falkowski PG (1984) Primary production and photoadaptation in light- and shade-adapted colonies of the symbiotic coral, *Stylophora pistillata*. Proc R Soc Lond B 222: 161-180.

34. Raven JA (1976) The rate of cyclic and non-cyclic photophosphorylation and oxidative phosphorylation, and regulation of the rate of ATP consumption in *Hydrodictyon africanum*. New Phytol 76: 205-212.

35. Revsbech NP, Jorgensen BB (1983) Photosynthesis of benthic microflora measured with high spatial resolution by the oxygen microprofile method. Limnol Oceanogr 28:749-756.

36. Streamer M, McNeil YR, Yellowlees D (1993) Photosynthetic carbon dioxide fixation in zooxanthellae. Mar Biol 115: 195-198.

37. Stumm W, Morgan JJ (1996) Aquatic Chemistry. John Wiley & Sons, Inc. USA.

38. Suzuki A, Nakamori T, Kayanne H (1995) The mechanism of production enhancement on coral reef carbonate systems: model and empirical results. Sed Geol 99: 259-280.

39. Tambutte E, Allemand D, Mueller E, Jaubert J (1996) A compartmental approach to the mechanism of calcification in hermatypic corals. J Exp Biol 199: 1029-1041.

40. Tayler EM, Trench RK (1986) Activities of enzymes in B-carboxylation reactions and of catalase in cell-free preparations from the symbiotic dinoflagellates Symbiodinium sp. from a coral, a clam, a zoanthid and two sea anemones. Proc R Soc Lond B 228: 483-492.

41. Walker D (1992) Excited leaves. NewPhytol 121: 325-345.

42. Wingler A, Lea PJ, Quick WP, Leegood RC (2000) Photorespiration: metabolic pathways and their role in stress protection. Phil T R Soc London B-Biol Sci 355(1402): 1517-1529.

43. Yamashiro H (1995) The effect of HEBP, an inhibitor of mineral deposition, upon photosynthesis and calcification in the scleractinian coral, *Stylophora pistillata*. J Exp Mar Biol Ecol 191:57-63.

44. Young SD, O´connor JD, Muscatine L (1971) Organic material from scleractinian coral skeletons-II. Incorporation of ^{14}C into protein, Chitin and lipid. Comp Biochem Physiol 40B: 945-958.

Chapter 4

Spatial distribution of calcification and photosynthesis in the scleractinian coral *Galaxea fascicularis*

Manuscript submitted for publication in Coral Reefs

Spatial distribution of calcification and photosynthesis in the scleractinian coral *Galaxea fascicularis*

Fuad A. Al-Horani[1, 2], Tim Ferdelman[1], Salim M. Al-Moghrabi[2], Dirk de Beer[1]
1. Max Planck Institute for Marine Microbiology, Celsiusstrasse 1, D-28359 Bremen, Germany
2. Marine Science Station, P. O. Box (195), Aqaba, 77110 Jordan

Abstract

The spatial heterogeneity of photosynthesis and calcification of single polyps of the coral *Galaxea fascicularis* was investigated. Photosynthesis was investigated with oxygen microsensors. The highest rates of gross photosynthesis (Pg) were found on the tissue covering the septa, the tentacles and the tissues surrounding the mouth opening of the polyp. Lower rates were found on the tissues of the wall and the coenosarc. Calcification was investigated by radioactive tracers. The incorporation pattern of ^{45}Ca and ^{14}C in the corallites was imaged with use of a Micro-Imager. The β-images obtained showed that the incorporation of the radioactive tracers coincided with the Pg distribution pattern with the highest incorporation rates found in the corallite septa. Thus, the high growth rate of the septa is supported by the high rates of Pg by the symbiont in the adjacent tissues. The total incorporation rates were higher in light than in dark, however, the distribution pattern of the radioisotope incorporation was not affected by illumination. This further emphasizes the close relation between calcification and photosynthesis.

Introduction

Scleractinian corals are $CaCO_3$ skeletons covered by thin layer of tissue. The colonies they form are made up of smaller building blocks, the polyps. The thin layer of tissue is composed of two epithelia separated by the body cavity, the coelenteron. The $CaCO_3$ skeleton underneath the tissue layer is secreted by the animal and its shape is characteristic at the species level (Fig. 1). The corals have symbiotic relationship with *Symbiodinium sp.* embedded in its endodermal cells. It has been long known that the rate of coral calcification is higher in light than in dark (e.g. Goreau, 1959; Pears & Muscatine, 1971; Chalker and Taylor 1975). This light enhancement of calcification was attributed to photosynthesis by the symbiont, though the exact

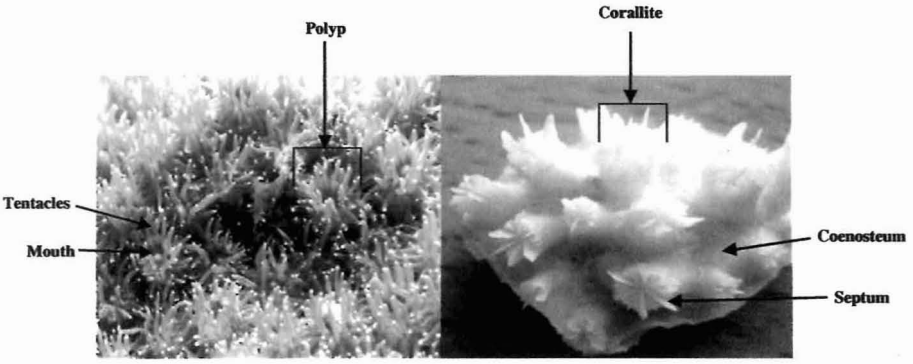

Fig. 1: Digital photographs of a *G. fascicularis* colony showing the heterogeneous polyps (left) and corallites (right).

mechanism of this enhancement yet is not very well established (see reviews by Barnes and Chalker 1990; Allemand et al. 1998; Gattuso et al. 1999).

The overall coral shape is determined by the differential growth rates of its building blocks. Goreau (1959) noticed variation in the growth rates of the different parts of the coral colony. Furthermore, Marshall and Wright (1998) found that different parts of the polyp incorporate ^{45}Ca and ^{14}C differently. Similarly, it has been shown with microsensors that photosynthesis and calcium dynamics are heterogeneous on the coral surface (Kühl et al. 1995; De Beer et al. 2000). Yet, a study of the interactions between the symbiont photosynthesis and the animal calcification at a microscale level is still lacking. We have combined oxygen microsensors and Micro-Imager (both with ca. 10 μm spatial resolution) to study the rates of photosynthesis and calcification on the different parts of the coral *G. fascicularis* polyps. With this study we try to relate the heterogeneous polyp surface with its physiology. The effect of light, dark and isotopic exchange on the incorporation of ^{45}Ca, ^{14}C-labelled bicarbonate and glucose were also studied.

Materials and Methods

Biological samples

Galaxea fascicularis colonies originated from the gulf of Aqaba-Jordan were transferred to Max Planck Institute, Bremen-Germany. They were maintained in aquarium (35‰ salinity, pH around 8.2, light intensity of 140-170 μmole photons m^{-2} s^{-1}, temperature of 26°C). Single polyps were fixed on small glass vials with underwater epoxy and left in the aquarium until a microcolony was developed and used in the incubation experiments.

Measurement of photosynthesis

Clark type O_2 electrodes (Revsbech and Jorgensen 1983) were used to measure gross photosynthesis using the light/dark shifts as described previously (Kühl et al. 1995). The coral colonies were placed in a polycarbonate flow cell for microsensor measurements. Filtered seawater was circulated between the flow cell and a 3 L reservoir at a constant flow rate (450 ml/min). The reservoir was continuously aerated. Motorized micromanipulators fixed on a heavy stand were used to position the electrodes on different parts of the polyps. A halogen light source (KL 1500 Schott Mainz company-Germany) provided a light intensity of 170-μmole photons m^{-2} s^{-1}.

Incubation with radioactive tracers

Coral colonies were incubated in a beaker containing 400 ml of filtered artificial seawater prepared from tropical marine salt (35 ‰ salinity pH of 8.2). The water was stirred and the temperature was maintained at 26°C. The incubation period was 5 hrs in all the experiments. Prior to addition of the radiotracer, the coral pieces were left for at least 1hr to recover from the transfer and acclimatize in the incubation conditions. Radioactive tracers, ^{45}Ca as $CaCl_2$, ^{14}C-glucose and ^{14}C-HCO_3^- (Amersham Pharmacia Biotech, UK) were added to a final activity of 3 KBq/ml in all the experiments. The specific activities were 74.0 MBq/ml for calcium, 2.0 GBq/mmol for bicarbonate and 12.0 GBq/mmol for glucose.

Two experimental conditions were applied; the first is illumination with 170-μmole photons m^{-2} s^{-1}, and second is dark incubations. Controls for isotopic exchange were done with killed specimens by 2% formaldehyde.

Processing of the samples after incubation

After the incubation, the coral colonies were extensively washed in 2 L filtered seawater (two successive times, 5 min. each). After washing, single polyps were separated from the mother colony by wire cutter. The skeletons that were not covered with tissue were discarded. After that, the colonies and the polyps were heated in 2N NaOH at 90°C for 20 minutes to hydrolyze the tissue. The skeletons were washed several times with NaOH solution to remove the tissue within the corallite. Decay per minute (dpm) in the hydrolysate was determined using a Packard TR 2500 scintillation counter operating in efficiency tracing mode to correct for quench. The skeletons were then washed with distilled water to remove nonspecifically bound tracer and dried at 50°C overnight. The next day, the skeletons incubated in ^{45}Ca were weighed and hydrolyzed in 12N HCl solution and the activity was counted. CO_2-trapping (for the colonies labeled with ^{14}C) was done according to the method of Boetius et al (2001) with slight modification after T. Treude (in preparation).

In another set of experiments, skeletons from the previous experiments were immersed in epoxy resin for β-Imaging. After two days in the resin, a diamond rock saw (CONRAD D 33892 CLAUSTHAL-ZELLERFELD rock saw) was used to make 2 mm thick longitudinal slices of the corallites.

β-Imaging

Autoradiography of the coral slices were acquired in 12 hrs exposure (fixed time for all the samples) in a Micro-Imager equipped with an intensified charge-coupled device (CCD) as described in Lanience et al., (1998). Briefly, each coral slice was positioned on a microscopic slide and covered with a scintillating sheet. The device allows 10-15μm spatial resolution. The accompanying software allows quantification of the images.

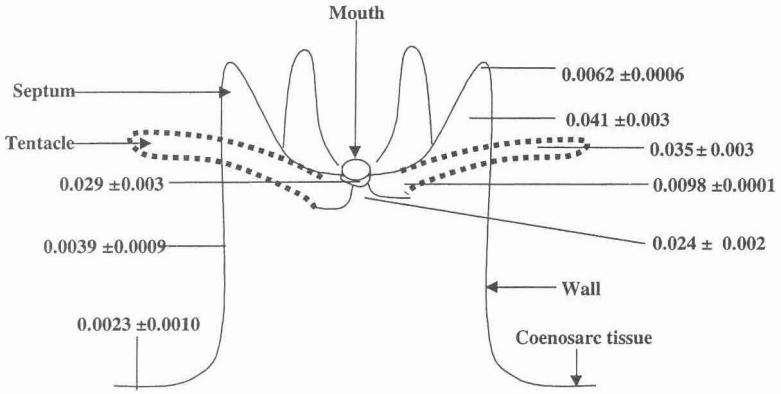

Fig. 2: Schematic drawing of a *G. fascicularis* polyp showing the rates of gross photosynthesis measured at the sites specified. The rates are expressed in mole O_2 m^{-3} s^{-1}.

A digital camera was used to photograph the coral slices to be compared with the images developed by the Micro-Imager.

Results

Gross photosynthesis (Pg) was very heterogeneously distributed over a single polyp. The rates of Pg were found highest on the top parts of the *G. fascicularis* polyp (Fig. 2). The tissue covering the base of the septum and the middle piece of the tentacles had rates of 0.041 ± 0.003 moles O_2 m^{-3} s^{-1} and 0.035 ± 0.003 moles O_2 m^{-3} s^{-1}, respectively. However, the very tips of the septa had a very low Pg rate. The mouth and adjacent tissue had Pg rates ranging from 0.024 ± 0.002 – 0.029 ± 0.003 (ca. 60-70% of the rates on the septum and the tentacle). Pg in the tissue covering the wall of the polyp was 10% of that of the septum and tentacle. The lowest Pg rate was found on the coenosarc (the tissue connecting adjacent polyps).

Also ^{45}Ca incorporation was very heterogeneous. The coral corallites septa incorporated more ^{45}Ca than the bottom parts in both light and dark as indicated by the β-images and the β-counts of the slices (Fig. 3). The light incubated colonies had ca. 58% higher ^{45}Ca incorporation rate in its skeletons compared to the dark incubated ones (Fig. 4). The rate of calcification is

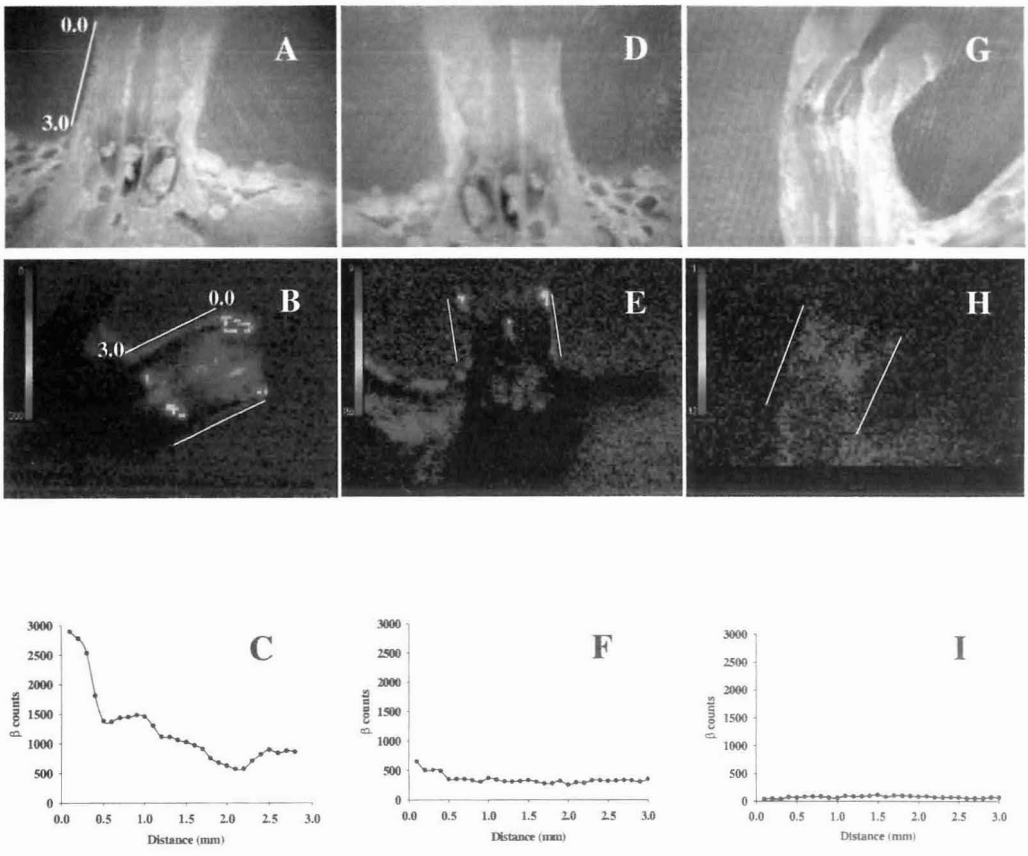

Fig. 3: Results from the Micro-Imager for the *G. fascicularis* colonies incubated with ^{45}Ca. A. Digital photo of a longitudinal slice of corallite after incubation in light, B. β-image of the slice in A, C. β-count of the image in B starting from top to bottom of the image, D. Digital photo of a longitudinal slice of corallite after incubation in dark, E. β-image of the slice in D, F. β-count of the image in E starting from top to bottom of the image, G. Digital photo of a longitudinal slice of corallite killed with 2% formaldehyde, H. β-image of the slice in G, I. β-count of the image in H starting from top to bottom of the image. The β-counts (C, F, I) were done for the cross sectional area over distance between the two lines in the corresponding images (B, E, H).

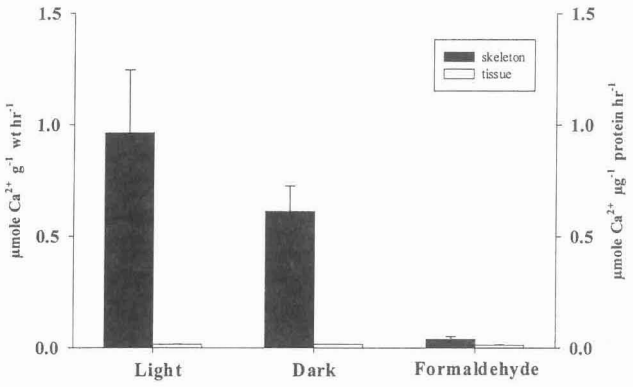

Fig. 4: ^{45}Ca incorporation in the skeleton and the tissue fractions of *G. fascicularis* after incubation in light, dark and in the presence of 2% formaldehyde. The Y-axis to the left is for skeleton values and one to the right is for tissue values

0.96 ± 0.28 µmole Ca^{2+} g^{-1} skeleton weight h^{-1} in light and 0.61 ± 0.11 µmole Ca^{2+} g^{-1} skeleton weight h^{-1} in dark.

Skeletons of the dead colonies incorporated 4-6% of the tracer relative to the living colonies. Only a background activity image was obtained upon imaging of the corallite slices of the dead colonies (Fig. 3).

The tissue fraction had very little ^{45}Ca incorporation in both light and dark conditions. The rate of incorporation is ca. 0.016 ± 0.002 µmole Ca^{2+} μg^{-1} protein hr^{-1} and ca. 0.016 ± 0.0004 µmole Ca^{2+} μg^{-1} protein hr^{-1} in light and dark incubations, respectively. About 85% (ca. 0.014 ± 0.002 µmole Ca^{2+} μg^{-1} protein hr^{-1}) relative to the tissue fractions of the living colonies was found in the tissue fraction of the dead colonies (Fig. 4).

Heterogeneity was also observed when the coral colonies were incubated in $^{14}C\text{-}HCO_3^-$ (Fig. 5). The β-images of the corallites` slices and β-counts revealed that the septa incorporated

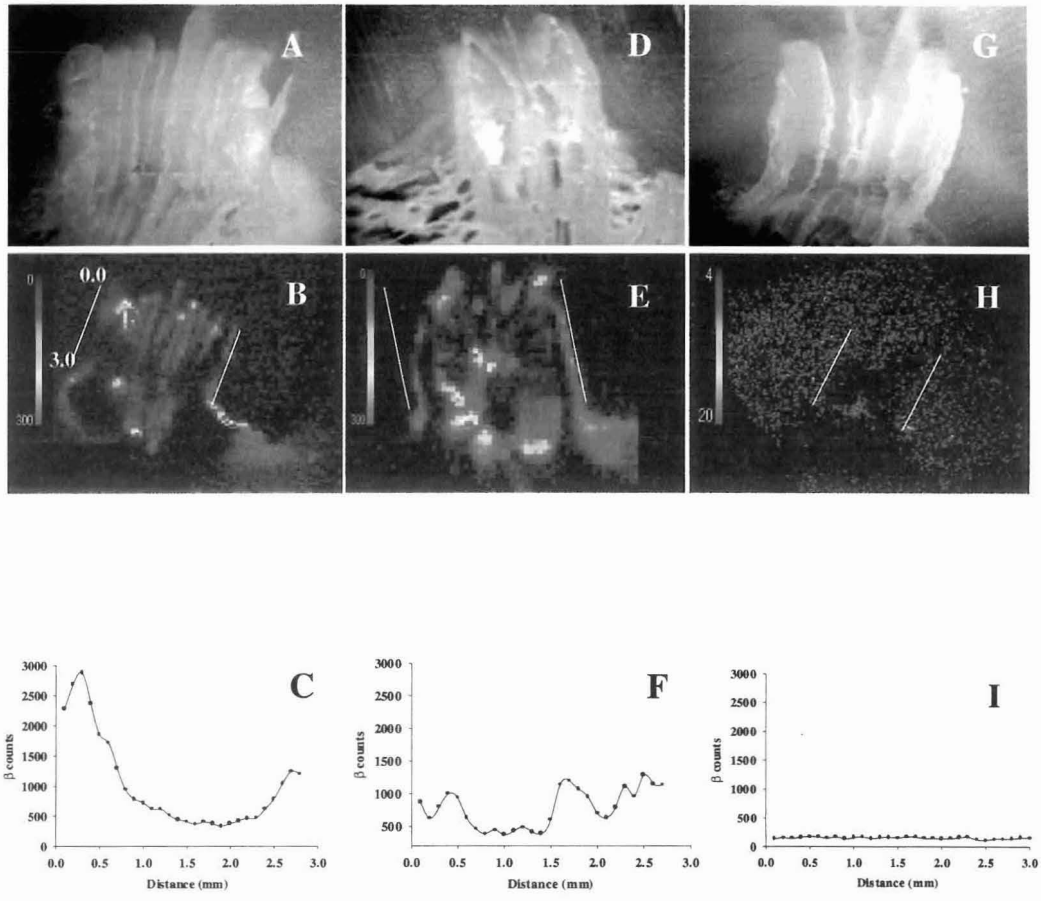

Fig. 5: Results from the Micro-Imager for the *G. fascicularis* colonies incubated with $^{14}C\text{-}HCO_3^-$. A. Digital photo of a longitudinal slice of corallite after incubation in light, B. β-image of the slice in A, C. β-count of the image in B starting from top to bottom of the image, D. Digital photo of a longitudinal slice of corallite after incubation in dark, E. β-image of the slice in D, F. β-count of the image in E starting from top to bottom of the image, G. Digital photo of a longitudinal slice of corallite killed with 2% formaldehyde, H. β-image of the slice in G, I. β-count of the image in H starting from top to bottom of the image. The β-counts (C, F, I) were done for the cross sectional area over distance between the two lines in the corresponding images (B, E, H).

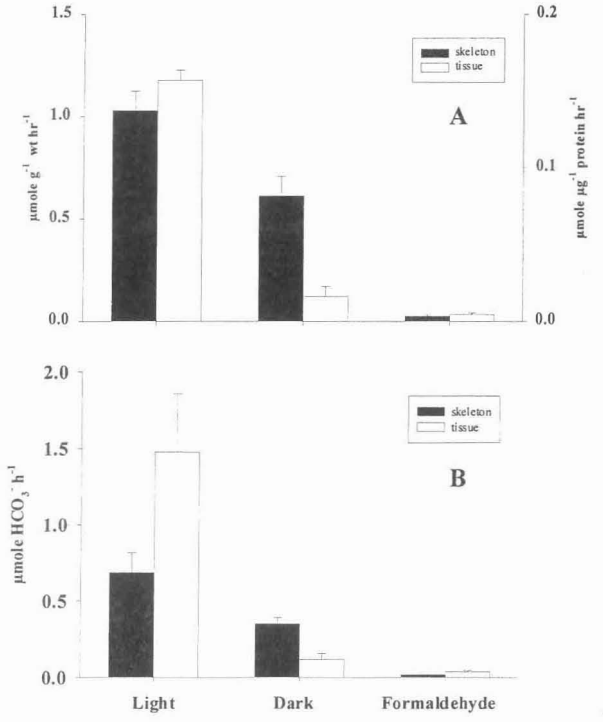

Fig. 6: (A) Incorporation of ^{14}C in the skeleton and tissue fractions of *G. fascicularis* incubated with ^{14}C-HCO_3^- in light, dark and in the presence of 2% formaldehyde, the Y-axis to the left is for skeleton values and one to the right is for tissue values. (B) Distribution of the total tracer incorporated between the skeleton and tissue fractions.

most of the radioactive tracer. The corallites incorporated the tracer ca. 67% higher in light compared to dark (Fig. 6A). The rate of calcification depending on ^{14}C-HCO_3^- incorporation is 1.03 ± 0.09 µmole HCO_3^- g^{-1} skeleton weight h^{-1} and 0.61 ± 0.09 µmole HCO_3^- g^{-1} skeleton weight h^{-1} in light and dark, respectively. Only 2.5% and 4.1% of the tracer relative to the living colonies incubated in light and dark, respectively, was incorporated in the corallites of the formaldehyde treated colonies. The β-image of this treatment showed only a background activity in the corallite slice (Fig. 5).

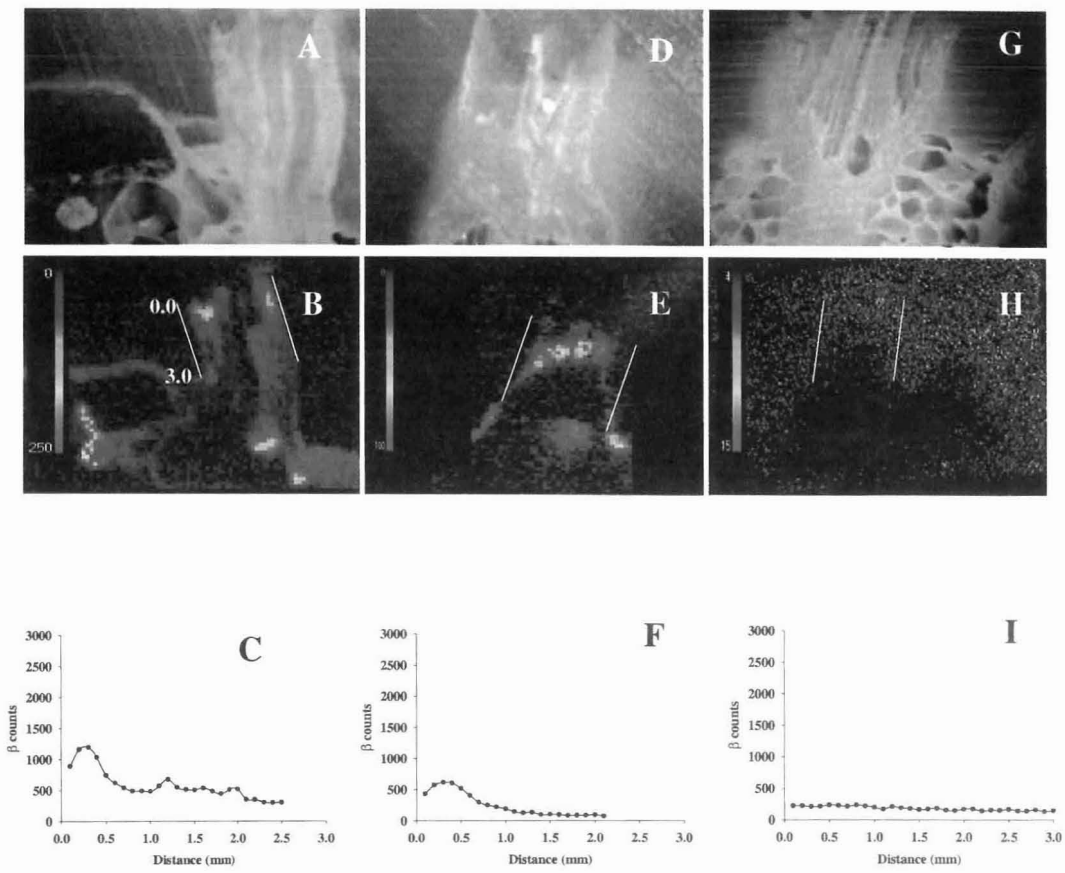

Fig. 7: Results from the Micro Imager for the *G. fascicularis* colonies incubated with ^{14}C-glucose. A. Digital photo of a longitudinal slice of corallite after incubation in light, B. β-image of the slice in A, C. β-count of the image in B starting from top to bottom of the image, D. Digital photo of a longitudinal slice of corallite after incubation in dark, E. β-image of the slice in D, F. β-count of the image in E starting from top to bottom of the image, G. Digital photo of a longitudinal slice of corallite killed with 2% formaldehyde, H. β-image of the slice in G, I. β-count of the image in H starting from top to bottom of the image. The β-counts (C, F, I) were done for the cross sectional area over distance between the two lines in the corresponding images (B, E, H).

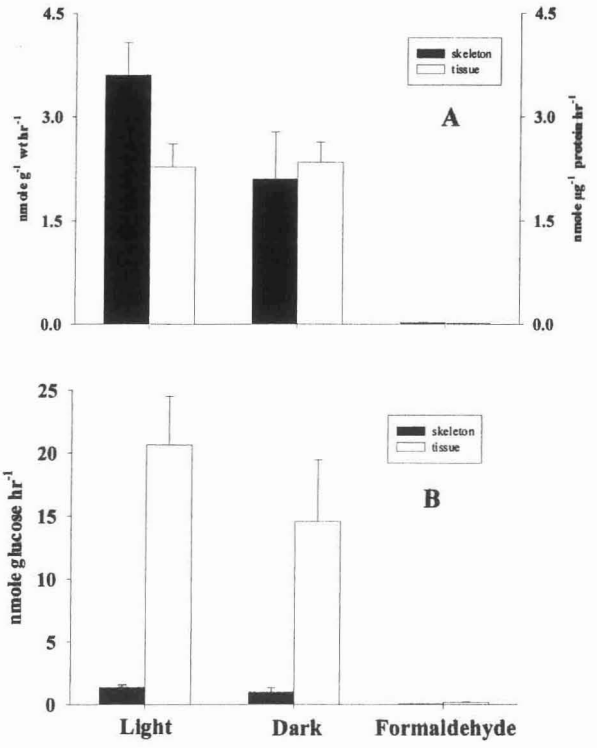

Fig. 8: (A) Incorporation of ^{14}C in the skeleton and tissue fractions of *G. fascicularis* incubated with ^{14}C-glucose in light, dark and in the presence of 2% formaldehyde, the Y-axis to the left is for skeleton values and one to the right is for tissue values. (B) Distribution of the total tracer incorporated between the skeleton and tissue fractions.

The ^{14}C-HCO_3^- tracer incorporation in tissue fraction is ca. 10 times higher in light than in dark (Fig. 6A). The rate of tracer incorporation is 0.160 ± 0.007 µmole HCO_3^- μg^{-1} protein h^{-1} and 0.016 ± 0.006 µmole HCO_3^- μg^{-1} protein h^{-1} in light and dark, respectively. The tissue fraction of the dead colonies had ca. 2.8% and 27% tracer incorporation, relative to the living colonies incubated in light and dark, respectively.

The total ^{14}C-HCO_3^- tracer incorporation in the skeleton and tissue fractions is about 4x higher in light than in dark (Fig. 6B). In light, ca. 32% of the total tracer incorporation was

found in the skeleton and ca. 68% in the tissue. In dark, ca. 75% of the tracer was found in the skeleton fraction and only 25% in the tissue fraction.

Incubation with ^{14}C-labelled glucose showed similar trend in the radioactive tracer incorporation in the corallites with the top parts being more active in the tracer incorporation in light and dark conditions (Fig. 7). The corallites were more active in the tracer incorporation in light than in dark. The dark incubated colonies incorporated ca. 58% of the tracer in their skeletons relative to the light incubated colonies (Fig. 8A). The dead colonies incubated in the presence of 2% formaldehyde did not incorporate the tracer in their skeletons and only a background image was observed upon imaging (Fig. 7). Only 0.6% and 1.1% tracer incorporation relative to the light and dark incubated colonies, respectively were found in the skeletons of the dead colonies (Fig. 8A).

Illumination had little effect on the rates of ^{14}C-glucose incorporation in the coral tissue and similar incorporation rates in both light and dark conditions were obtained (Fig. 8A). The rate is 2.28 ± 0.33 nmole glucose μg^{-1} protein h^{-1} and 2.34 ± 0.23 nmole glucose μg^{-1} protein h^{-1} in light and dark, respectively. The dead colonies incubated in 2% formaldehyde incorporated only 0.5% of the tracer in their tissue fractions relative to the living colonies.

Coral tissue incorporated ^{14}C from glucose more actively than the skeleton. In both light and dark conditions, 6% of the radioactive tracer was found in the skeleton fraction, while 94% was found in the tissue fraction (Fig. 8B). The total ^{14}C-glucose incorporation in the two fractions was ca. 40% higher in light than in dark.

Discussion

Oxygen production in *Galaxea fascicularis* was found to be highly heterogeneous on the surface of their polyps (Fig. 2). The rate of gross photosynthesis (Pg) was found highest on the tissue covering the middle parts of the corallite septa, the tentacles and the tissue surrounding the mouth of the polyp. The tissues covering the white tips of the septa, the wall of the polyp and the coenosarc (the tissue that connects polyps in the colony) had ca. 1 order of magnitudes lower Pg rates.

The main product of photosynthesis is the reduced organic carbon compounds. In corals, most of the organic carbon compounds produced by the zooxanthellae are transported to the animal (Muscatine et al., 1981; Muscatine et al. 1984). This can be used as energy reservoir as well as building blocks during biosynthesis in the polyp. On the other hand, the oxygen produced during photosynthesis helps maintining oxic condition in the coral. Both products, reduced carbon compounds and oxygen, are used in production of ATP, which is required by calcification. Thus, the high rates of Pg in the top parts of the coral polyp indicate high rates of energy and organic carbon production in those polyp parts.

The rate of Pg in corals is dependant on the number and activity of zooxanthellae and the light field in the spot measured. The spatial distribution of zooxanthellae and the cell specific density (number of zooxanthellae per host cell) on the polyp surface is determined by the tissue architecture and the general colony morphology (Helmuth et al. 1997; Muscatine et al. 1998). The efficiency of light capturing is influenced by the polyp shape (Porter, 1976). It was found by Kühl et al. (1995) that the light field at the tissue surface of the coral differs strongly with respect to intensity and spectral composition. Thus, the zooxanthellae productivity differs in the different localities on the coral surface as it is reflected by the heterogeneous distribution of Pg rates. This in turn will strongly affect the coral metabolism in the vicinity of the adjacent polyp parts. The more the energy and organic carbon produced, the higher can the growth rates be of the connected polyp parts.

When *G. fascicularis* colonies were incubated in the presence of ^{45}Ca, the radioactive tracer incorporation into the coral corallites was not homogeneous (Fig. 3). The corallites incorporated more ^{45}Ca in its highermost parts, specifically the tips of the septa, compared to the lower parts, the walls and the coenosteum (the skeletal material between the corallites). The •-count of the corallite image in light showed a steep decrease in the activity from top to bottom of the •-image (Fig. 3). This indicates differences in calcification rates among those parts of the polyp. The results are consistent with the findings of Marshall and Wright (1998) where they have shown that the ^{45}Ca was incorporated differently in the cross sections of coral corallite. Both light incubated and dark incubated colonies showed similar pattern of ^{45}Ca incorporation, although the overall ^{45}Ca incorporation is higher in light than in dark (Fig. 4). This suggests that the distribution pattern of calcification on the corallite surface is morphogenetically determined

rather than being affected by the light field. Based on ^{45}Ca uptake, the calcification rate in light is close to 1 μmole g^{-1} skeleton weight hr^{-1}, a rate that lies within the range reported for other scleractinian corals (Erez, 1978). This rate is about 58% higher than dark calcification, which confirms previous observations in corals (e.g. Goreau 1959).

Calcification in corals was shown to be an energy demanding process (Chalker and Taylor 1975; Krishnaveni et al. 1989; Tambutte et al. 1996). Thus, the higher rates of calcification in the top parts of the polyp necessitates a higher rates of energy supply to those parts. The high energy demand for those parts is possibly supplied through the high rates of photosynthesis in the adjacent polyp parts. Although the very tips of the septa showed low rates of Pg, reduced organic carbon compounds produced by zooxanthellae in the lower tissues can be translocated to the growing tips where ATP can be generated for calcification (Pears and Muscatine 1971; Fang et al. 1989).

Although the use of radioactive isotopes in studying coral calcification started some fifty years ago (Goreau 1959), estimation of isotopic exchange remained a problem (Tambutte et al. 1996). Error associated with isotopic exchange were reduced by using cultured microcolonies with no skeletons exposed to the radioisotope-labelled incubation medium (Tambutte et al. 1995), but it is still dificult to distiguish isotopic exchange from dark calcification (Chalker and Taylor 1975; Marshall and Wright 1998). To distinguish the difference between isotopic exchange and dark calcification, colonies were killed with 2% formaldehyde and incubated in a similar way like the living colonies. In this way, we could exclude all the biological factors without removing the tissue layer, which help forming a barrier for isotopic exchange (Goreau 1959). The results showed a large difference between the dark incubated colonies and the dead ones, with much higher tracer incorporation in the dark incubated colonies compared to the dead colonies. Thus, dark calcification does indeed exist and is not an artifact of isotopic exchange.

The tissue fraction did not incorporate ^{45}Ca in both light and dark incubated colonies. The coral colonies had incorporated ca. 0.016 μmole Ca^{2+} μg^{-1} protein hr^{-1} Only 1-2% in their tissue fractions under both light and dark conditions (Fig. 4). This is similar to the amount of tracer found in the tissue fraction of the dead colonies, indicating that only physical diffusion of the tracer is reponsible for it rather than being incorporation into the tissue. With the radioactive

tracer method, it is not possible to evaluate whether an active transport system exists in the tissue or not, the animal tissue maintains very low intracellular Ca^{2+} concentrations (Barnes and Chalker, 1990). Other methods are required such as microsensor methods to demonstrate the presence of an active transport mechanism for Ca^{2+} ions (Al-Horani et al. in preparation).

The incorporation pattern of ^{14}C-HCO_3^- into the coral corallites was similar to that of ^{45}Ca incorporation (Fig. 5). The corallite septa were more active in the tracer incorporation in both light and dark incubations. The ratio of light to dark incorporation of the ^{14}C-HCO_3^- tracer was close to that of ^{45}Ca. Based on ^{14}C-HCO_3^- uptake, the rate of calcification is ca. 1.03 μmole HCO_3^- g^{-1} skeleton weight hr^{-1}, a value close to that calculated from ^{45}Ca uptake. The rate in dark is the same as that obtained with ^{45}Ca uptake giving a stoichiometric ratio of 1:1 for calcium and carbon uptake in the coral $CaCO_3$ skeleton. The dead colonies did not incorporate the ^{14}C tracer into their skeletons confirming the results obtained with ^{45}Ca.

A main difference between the ^{14}C-HCO_3^- and ^{45}Ca incorporation was observed in the tissue incorporation of the tracer. About 68% of the total incorporated ^{14}C-HCO_3^- tracer in the whole colony was found in the tissue fraction in light (Fig. 6B). Under dark condition, only 25% of the total incorporation of ^{14}C-HCO_3^- tracer was found in the tissue fraction, while 75% was found in the skelton fraction. Obviously, photosynthesis is the main process responsible for the HCO_3^- incorporation in the tissue in light. Active transport of HCO_3^- may be involved in the dark incorporation of the HCO_3^- (Furla et al. 2000). The total ^{14}C-HCO_3^- incorporation in both tissue and skeleton increased 4 folds in light, which strongly suggests that no competition between photosynthesis and calcification for dissolved inorganic carbon exists.

In another set of experiments, ^{14}C-labelled glucose was added to the incubation medium as an external energy and carbon source. Although glucose is normaly present in low concentrations in the sea, the corals are efficient in using it as energy source (Stephens 1960). The data showed that *G. fascicularis* incorporates the ^{14}C tracer from glucose in its skeletons and tissues in both light and dark conditions. The pattern of incorporation into the corallite is similar to the incorporation of the ^{45}Ca and ^{14}C-HCO_3^- with the top part being more active in incorporating the tracer (Fig. 7).

In the corallites, the incorporation of ^{14}C from glucose was higher in light than in dark. This could be attributed to the enhanced rates of coral calcification and respiration in light (Chalker and Taylor 1975; Kühl et al. 1995). Because the use of glucose is dependant on the respiration efficiency, the respiration in dark is limited by the diffusive supply of oxygen through the diffusive boundary layer (Kühl et al. 1995), while in light, photosynthesis creates oxic environment in the coral, thereby enhancing respiration. The incorporation of ^{14}C from HCO_3^- and glucose into the coral skeleton is consistent with the hypothesis that both carbon sources are used in coral calcification (Goreau 1977; Erez 1978).

Unlike the incorporation of ^{45}Ca and ^{14}C-HCO_3^-, most of the ^{14}C-glucose incoporated in the coral was found in the tissue fraction in both light and dark conditions (Fig. 8B). In both light and dark conditions, about 94% of the total incorporated ^{14}C-glucose tracer was found in the tissue fraction, while only 6% was found in the skeleton fraction. This is consistant with the study by Anthony and Willis (in process) that corals invest more energy in tissue growth than in skeletal growth. Glucose incorporation into the tissue was not affected by the light condition, suggesting that it is not a light dependant process.

There was no isotopic exchange in the case of ^{14}C-glucose incubation in both skeleton and tissue fractions in light and dark incubations. The very small amount of the tracer (0.6-1.1% of the total incorporation relative to the living colonies) found in the tissue and skeleton of the dead colonies can be attributed to nonspecific binding. In the case of ^{14}C-HCO_3^-, 2.5% and 4.1% of the tracer incorporation in the skeleton in light and dark, respectively, is attributed to isotopic exchange. These values should be considered for the estimation of calcification rates in corals when using radioactive tracers.

Conclusion

The coral display heterogeneous growth rates of the corallite parts. The highest growth rate was found in the septa, while lower rates were found on the corallite wall and the coenosteum. This differential growth rate is supported by symbiont photosynthesis, which display similar distribution pattern on the polyp surface.

The distribution pattern of the radioisotopes (^{45}Ca and ^{14}C) in the corallite was similar in light and dark suggesting that it is a morphogenetically controlled process, although the rate of incorporation was high in light compared to dark.

The ^{45}Ca was incorporated solely in the corallite skeleton, while ^{14}C-HCO_3^- was incorporated in the skeleton and the tissue fractions. The incorporation of ^{45}Ca and ^{14}C-HCO_3^- in the coral skeleton was enhanced during light incubation. The rate calculated gave a stoichiometric ratio of 1:1 based on incorporation of the two tracers.

The ^{14}C-glucose was incorporated in both skeleton and tissue fractions of the coral. Most of the ^{14}C-glucose incorporated was found in the tissue fraction. The tissue incorporation of the tracer was not affected by illumination condition.

The use of killed colonies allowed estimation of the isotopic exchange between the coral skeleton and the surrounding incubation medium. The use of such colonies allows estimation of the actual calcification in light and dark.

Acknowledgements

This study was funded by Max Planck Institute for Marine Microbiology-Bremen, Germany. We thank G. Eickert, A. Eggers and I. Schröder for constructing the oxygen electrodes, S. Rousan (from university of Bremen) and N. Finke, H. Jonkers (from the MPI-Bremen) for technical support. We also thank the staff of the Marine Science Station in Aqaba-Jordan for supplying the diving equipments, Laboratory space and coral specimens.

Reference

1. Allemand D, Furla P, Benazet-Tambutte S (1998) Mechanisms of carbon acquisition for endosymbiont photosynthesis in Anthozoa. Can J Bot. 76: 925-941

2. Anthony KRN, Willis BL. Skeletal growth rate: a poor indicator of coral energy investment? (In process).

3. Barnes DJ, Chalker BE (1990) Calcification and photosynthesis in reef-building corals and algae. In Z. Dubinsky (ed.), Coral reefs. pp. 109-131. Elsevier, Amsterdam.

4. Boetius A, Ferdelmann T, Lochte K (2001) Bacterial activity in sediments of the deep Arabian Sea in relation to vertical flux. Deep-Sea Res. II 47: 2835-2875

5. Chalker BE, Taylor DL (1975) Light-enhanced calcification, and the role of oxidative phosphorylation in calcification of the coral *Acropora cervicornis*. Proc R Soc London B 190: 323-331

6. De Beer D, Kühl M, Stambler N, Vaki L (2000) A microsensor study of light enhanced Ca^{2+} uptake and photosynthesis in the reef-building hermatypic coral *Favia* sp. Mar Ecol Prog Ser 194:75-85

7. Dubinsky Z, Stambler N, Ben-Zion M, McCloskey L, Muscatine L, Falkowski PG (1989) The effect of external nutrient resources on the optical properties and photosynthetic efficiency of Stylophora pistillata. Proc R Soc London B 239: 231-246

8. Erez J (1978) Vital effect on stable-isotope composition seen in foraminifera and coral skeletons. Nature 273: 199-202

9. Fang LS, Chen YWJ, Chen CS (1989) Why does the white tip of stony coral grow so fast without zooxanthellae? Mar Biol. 103: 359-363

10. Furla P, Benazet-Tambutte S, Allemand D, Jaubert J (1998) Diffusional permeability of dissolved inorganic carbon through the isolated oral epithelial layers of the sea anemone, *Anemonia viridis*. J Exp Mar Biol Ecol. 221: 71-88

11. Furla P, Galgani I, Durand I, Allemand D (2000) sources and mechanisms of inorganic carbon transport for coral calcification and photosynthesis. J Exp Biol. 203: 3445-3457

12. Gattuso JP, Allemand D, Frankignoulle M (1999) Photosynthesis and calcification at cellular, organismal and community levels in coral reefs: a review on interaction and control by carbonate chemistry. Am Zool. 39: 160-183

13. Goreau TF (1959) The physiology of skeleton formation in corals. I. A method for measuring the rate of calcium deposition by corals under different conditions. Biol Bull. 116: 59-75

14. Goreau TF (1963) Calcium carbonate deposition by coralline algae and corals in relation to their roles as reef-builders. Ann N Y Acad Sci 109: 127-167.

15. Goreau TJ (1977) Coral skeletal chemistry: physiological and environmental regulation of stable isotopes and trace metals in *Montastrea annularis*. Proc R Soc London B. 196: 291-315

16. Helmuth BST, Timmerman BEH, Sebens KP (1997) Interplay of host morphology and symbiont microhabitat in coral aggregation. Mar Biol 130: 1-10

17. Krishnaveni P, Chou LM, Ip YK (1989) Deposition of calcium (45Ca) in the coral, *Galaxea fascicularis*. Comp Biochem Physiol 94A: 509-513

18. Kühl M, Cohen Y, Dalsgaard T, Jorgensen BB, Revsbech NP (1995) Microenvironment and photosynthesis of zooxanthellae in scleractinian corals studied with microsensors for O_2, pH and light. Mar Ecol Prog Ser 117:159-172.

19. Laniece P, Charon Y, Cardona A, Pinot L, Maitrejean S, Mastrippolito R, Sandkamp B, Valentin L (1998) A new high resolution radioimager for the quantitative analysis of radiolabelled molecules in tissue section. J Neuroscience Meth 86:1-5

20. Marshall AT, Wright A (1998) Coral calcification: autoradiography of a scleractinian coral *Galaxea fascicularis* after incubation in ^{45}Ca and ^{14}C. Coral Reefs. 17: 37-47

21. Muscatine L, Falkowski PG, Porter JW, Dubinsky Z, (1984) Fate of photosynthetic fixed carbon in light- and shade-adapted colonies of the symbiotic coral, *Stylophora pistillata*. Proc. R. Soc. London B 222: 181-202

22. Muscatine L, Ferrier-Pages C, Blackburn A, Gates RD, Baghdasarian G, Allemand D (1998) Cell-specific density of symbiotic dinoflagellates in tropical anthozoans. Coral Reefs. 17: 329-337

23. Muscatine L, McCloskey LR, Marian RE (1981) Estimating the daily contribution of carbon from zooxanthellae to coral animal respiration. Limnol Oceangr. 26(4): 601-611

24. Pears VB, Muscatine L (1971) Role of symbiotic algae (zooxanthellae) in coral calcification. Biol Bull. 141: 350-363

25. Porter JW (1976) Autotrophy, heterotrophy, and resource partitioning in Caribbean reef building corals. Am Nat. 110: 731-742

26. Revsbech NP, Jorgensen BB (1983) Photosynthesis of benthic microflora measured with high spatial resolution by the oxygen microprofile method. Limnol Oceanogr 28:749-756

27. Simkiss K, Wilbur KM (1989) Biomineralization: Cell biology and mineral deposition. Academic press, Inc. UK.

28. Stephens GC (1960) Uptake of glucose from solution by solitary coral, *Fungia*. Science 131: 1532

29. Tambutte E, Allemand D, Bourge I, Gattuso JP, Jaubert J (1995) An improved ^{45}Ca protocol for investigating physiological mechanisms in coral calcification. Mar Biol 122: 453-459

30. Tambutte E, Allemand D, Mueller E, Jaubert J (1996) A compartmental approach to the mechanisms of calcification in hermatypic corals. J Exp Biol 199: 1029-1041

Summary

Much of the global interest in coral reefs is because they are major features on the earth's surface of high ecological and economical importance. The scleractinian corals are the main components of the coral reefs. In the past, calcification by corals and other photosynthesizing organisms played a major role in converting most of the carbon in the biosphere into limestone. A functional linkage between calcification and photosynthesis must be involved, since photosynthesizing organisms account for most of the calcification. Thus, global carbon cycles and sedimentary geology cannot be understood without addressing how calcification and photosynthesis are linked.

It has been discovered that scleractinian corals calcify at a faster rate in light and that algal symbiosis is necessary for rapid calcification rates exhibited by corals. Since the discovery of this phenomenon 50 years ago, scientists were trying to understand the mechanism of calcification and the role of light and the symbiont in its enhancement in corals. It is still not very well understood.

This thesis addressed this problem. Since carbon is a common substrate for calcification and photosynthesis, the second chapter in this thesis studied the sources of carbon for the two processes and its pathways in the coral. The title of this study is "Microsensor Study of Photosynthesis and Calcification in the Scleractinian Coral, *Galaxea fascicularis*: active internal carbon cycle". In this study, small colonies of the scleractinian coral, *Galaxea fascicularis* were used. Microsensors for O_2, Ca^{2+} and pH together with use of specific metabolic inhibitors and carbon free seawater were applied. Gross photosynthesis (Pg) and net photosynthesis (Pn) were measured on the surface of the polyp. Light respiration (LR) was calculated from Pg and Pn. The Ca^{2+} and pH dynamics on the surface and inside the polyp's coelenteron were compared for the first time. The effect of light/dark and dark/light switches on Ca^{2+} and pH dynamics on the surface and inside the coelenteron were followed.

The results obtained showed that the coral has a Pg rate that is much higher than the Pn rate and that up to 90% of the oxygen produced by photosynthesis is consumed in metabolic respiration of the symbiont and the coral host. Thus, photosynthesis and respiration form an

internal carbon cycle within the coral. As the internal C-cycle is highly active, a large part of the Ci for calcification will pass through the metabolism of the symbiont. The cycle provides ATP for energy requiring processes in light. The inorganic carbon for photosynthesis and calcification can come from seawater (free Ci) and from respiration of plankton and photosynthates. Carbon from the different pools (e.g. tissue, skeleton, photosynthates, and the dissolved organic and inorganic carbon in seawater and in coral) can easily be exchanged. Thus it is very difficult to follow the fate of carbon from one pool. Three localities of the enzyme Carbonic Anhydrase were defined. One on the surface facing seawater and one on endodermal cells facing the coelenteron, while the third is intracellular. The enzyme in the different localities helps in the uptake of inorganic carbon for photosynthesis and calcification and is also functioning in internal pH regulation.

In the second study entitled "Mechanism of calcification and its relation to photosynthesis and respiration in the scleractinian coral *Galaxea fascicularis*", the mechanism of calcification and its relation to photosynthesis and respiration in, *Galaxea fascicularis*, was studied with microsensors for Ca^{2+}, pH and O_2 (Chapter 3). In this study, the energy budget of the coral in light and dark conditions was compared. The results showed that the coral has a higher energy production in light than in dark as it was deduced from the higher rate of respiration and ATP content in light when compared to dark.

The direct measurements of Ca^{2+} and pH dynamics on the surface, inside the polyp's coelenteron and under the calicoblastic layer showed that the Ca^{2+} concentrations decreased in light on the surface and in the coelenteron compartments and increased upon switching light off. Under the calicoblastic layer the opposite was observed. In light, the level of Ca^{2+} was lower on the surface than in seawater, and even lower inside the coelenteron. Under the calicoblastic layer, the concentration of calcium was ca. 0.5-1 mM higher than seawater. Thus Ca^{2+} can diffuse from seawater to the coelenteron, but metabolic energy is needed for the transport across the calicoblastic layer to the skeleton. The pH under the calicoblastic layer was alkaline compared to the surface and inside the coelenteron. Because of this, the aragonite saturation state under the calicoblastic layer has increased from ca. 3.2 in the dark to ca. 25 in the light, creating an excellent environment for calcification in light.

When Ruthenium Red (specific inhibitor of Ca-ATPase) was added, Ca^{2+} and pH dynamics were inhibited under the calicoblastic layer. This indicated that Ca-ATPase transports Ca^{2+} against its gradient in exchange for H^+ at the calicoblastic layer. Addition of DCMU (PSII inhibitor) completely inhibited photosynthesis. The calcium dynamics under the calicoblastic layer continued, however, they were less regular. The initial rates were maintained. Thus it was concluded that light and not energy generation triggers calcium uptake, however energy (mainly supplied from respiration of photosynthates) is also needed.

In the third study (Chapter 4), the interaction between photosynthesis and calcification was studied at a microscale levels with microsensors and micro-autoradiography. The title of this study is "Spatial distribution of calcification and photosynthesis in the scleractinian coral *Galaxea fascicularis*". The results of this study showed that the highest rates of gross photosynthesis (Pg) are found on the tissue covering the septa, the tentacles and the tissues surrounding the mouth opening of the polyp. Lower rates were found on the tissues of the wall and the coenosarc. Incubation of the coral colonies with radioactive tracers for calcium ions and carbonate showed that the distribution of calcification on the polyp surface coincides with the distribution of photosynthesis. Thus, the high growth rate of the polyp septa, which showed highest rate of tracer incorporation, is supported by the high rates of Pg by the symbiont in the adjacent tissues. The total incorporation rates were higher in light than in dark, however, the distribution pattern of the radioisotope incorporation was not affected by illumination indicating that it is a morphogenetically controlled process. This further emphasizes the close relation between calcification and photosynthesis.

The incorporation of ^{14}C from HCO_3^- and glucose in the coral skeleton again demonstrated that both organic and inorganic carbon sources are potentially used in coral calcification. It was also shown that the coral tissue incorporates the two tracers in light preferentially over the skeleton while ^{45}Ca is not incorporated at all in the tissue. This underlines the conclusion from Chapter 2 that the pools exchange.

The use of killed colonies in the incubation experiments helped in estimating isotopic exchange rate and better estimating the actual calcification rates occurring in corals. The use of

novel micro-analytical techniques (microsensors and β-imaging) allowed settling a classical scientific debate on the coupling of photosynthesis and calcification in a convincing way.

Zusammenfassung

Ein Großteil des globalen Interesses and Korallenriffen rührt daher, dass sie wesentlicher Bestandteil der Erdoberfläche und von hoher ökologischer und ökonomischer Bedeu-tung sind. Hauptbestandteil eines Korallenriffes sind die riffbildenden Steinkorallen. Die in der Vergangenheit durch Korallen und andere photosynthetisch aktive Organsimen bewirkte Calcifikation spielte eine zentrale Rolle in der Fixierung des Kohlenstoffs der Biosphäre in Form von Kalkstein. Dabei muss eine funktionelle Verbindung zwischen den Prozessen der Calcifikation und der Fotosynthese beteiligt sein, da fotosynthetisch aktive Organismen für den Hauptteil der Calcifikation verantwortlich sind. Es folgt daraus, daß der globale Kohlenstoffkreislauf und die Sedimentgeologie ohne die Kenntnis der Interaktion dieser beiden Prozesse nicht verstanden werden können.

Bereits lange bekannt ist, dass Steinkorallen im Licht höhere Calcifikationsraten erreichen und dass die Symbiose mit Algen für hohe Calcifikationsraten essenziell ist. Seit der Entdeckung dieser Phänomene vor 50 Jahren versuchen Wissenschaftler den Mechanismus der Calcifikation, die Rolle des Lichts und der symbiontischen Algen in ihrer Verstärkung dieses Prozesses zu erhellen. Bisher gelang dieses nur unzureichend.

Die vorliegende Arbeit beschäftigt sich mit diesem Gegenstand. Da der Kohlenstoff ein Substrat sowohl für die Calcifikation als auch für die Fotosynthese darstellt, wurden im Kapitel zwei dieser Arbeit zunächst die Quellen und Wege des Kohlenstoffs im Zusammen-hang mit diesen beiden Prozessen untersucht. Der Titel der Studie lautet "Microsensor Study of Photosynthesis and Calcification in the Scleractinian Coral, *Galaxea fascicularis*: active internal carbon cycle". In der Studie wurden kleine Kolonien der Steinkoralle *Galaxea fasci-cularis* verwendet. Eingesetzt wurden Mikrosensoren für O_2, Ca^{2+} und pH zusammen mit spezifischen Stoffwechselinibitoren und kohlenstofffreies Seewasser als Inkubationsme-dium. Auf der Oberfläche des Polypen wurden Brutto- (Pg) und Netto-Fotosyntheseraten (Pn) gemessen, welche zur Berechnung der Atmungsrate unter Licht (LR) herangezogen wurden. Die Studie ermöglichte zum ersten Mal auch den Vergleich der Dynamik von Ca^{2+}-Konzentrationen und pH-Werten zwischen äußerer Oberfläche und Coelenteron des Poly-pen. Der Effekt von Licht-

Dunkel- und Dunkel-Licht-Wechseln auf die Dynamik dieser Parameter konnte ebenso verfolgt werden.

Die Ergebnisse zeigen, dass die Koralle eine wesentlich höhere Pg als Pn aufweist und dass bis zu 90% des durch die Fotosynthese erzeugten Sauerstoffs von der Atmung der Symbionten und des Korallengewebes selbst verbraucht werden. Es ergibt sich daraus, dass Fotosynthese und Atmung in der Koralle einen internen Kohlenstoffkreislauf bilden. Da die Kopplung beider Vorgänge sehr eng ist, durchläuft ein Großteil des durch die Calcifikation fixierten anorganischen Kohlenstoffs somit den Metabolismus des Symbionten. Der Kreis-lauf dient zur Erzeugung von ATP für energiebedürftige Prozesse im Licht. Der für die Foto-synthese und die Calcifikation benötigte anorganische Kohlenstoff kann aus dem Seewasser (freier Ci) oder aus veratmetem organischen Kohlenstoff (aufgenommenes Plankton und Fotosytheseprodukte) gewonnen werden. Kohlenstoff aus den verschiedenen Quellen (z.B. Gewebe, Skelettstrukturen, Fotosytheseprodukte, gelöster organischer und anorganischer Kohlenstoff aus dem Seewasser und der Koralle) ist jedoch leicht austauschbar. Damit ist es sehr schwierig, den Verbleib von Kohlenstoff aus einem bestimmten Pool festzustellen. Für das Vorkommen des Enzyms Carboanhydrase konnten drei verschiedene Bereiche definiert werden. Ein Bereich stellt die dem Seewasser zugewandte Oberfläche dar, ein weiterer liegt bei den dem Coelenteron zugewandten endodermalen Zellen, während der dritte Bereich ein intrazelluläres Vorkommen darstellt. Das Enzym unterstützt in den verschiedenen Bereichen die Aufnahme anorganischen Kohlenstoffs für Fotosynthese und Calcification und trägt des weiteren zur internen pH-Regulation bei.

In einer zweiten Studie mit dem Titel "Mechanisms of calcification and its relation to photosynthesis and respiration in the scleractinian coral *Galaxea fascicularis*" wurde der Mechanismus der Calcifikation und seine Beziehung zu Fotosynthese und Atmung in *Ga-laxea fascicularis* mit Hilfe von Mikrosensormessungen von O_2, Ca^{2+} und pH untersucht (Kapitel 3). Hier wurden die Energiebilanzen der Koralle unter den Bedingungen von Licht und Dunkelheit verglichen. Die Ergebnisse zeigen, dass die Koralle unter Beleuchtung mehr chemische Energie produziert als in der Dunkelheit, was aus den höheren Raten von At-mung und ATP-Gehalt unter Beleuchtung (im Vergleich zu Proben nach Dunkelinkubation) gefolgert werden konnte.

Die direkte Messung der Dynamik von Ca^{2+}-Konzentrationen und pH auf der Oberfläche, innerhalb des Coelenterons des Polypen und unterhalb des kalkbildenden aboralen Ektoderms zeigte, dass die Konzentrationen von Ca^{2+} unter Beleuchtung sowohl nahe der Oberfläche als auch im Coelenteron abnahmen, in der Dunkelheit jedoch wieder anstiegen. Unterhalb des aboralen Ektoderms wurde der umgekehrte Vorgang beobachtet. Im Licht war die Konzentration von Ca^{2+} nahe der Oberfläche des Polypen, und in stärkerem Maße noch im Coelenteron, niedriger als im umgebenden Seewasser. Unterhalb des aboralen Ektoderms dagegen war die Konzentration von Ca^{2+} etwa 0,5 bis 1 mM höher als im Seewasser. Cal-cium kann somit vom umgebenden Seewasser durch diffusiven Transport in das Coelenteron gelangen, während für den Transport über das aborale Ektoderm hinweg zum Kalkskelett Stoffwechselenergie erforderlich ist. Der pH-Wert unterhalb des aboralen Ektoderms war im Vergleich zur Oberfläche und zum Coelenteron alkalisch. Daraus ergibt sich, dass der Sättigungszustand von Aragonit unterhalb des aboralen Ektoderms von etwa 3,2 in Dunkelheit auf circa 25 im Licht zunimmt, was hervorragende Umgebungbedingungen für die Calcifika-tion im Licht erzeugt.

Eine Zugabe von Ruthenium-Rot, einem Inhibitor für die Ca-ATPase, führte zu einem Zusammenbruch der Dynamik von Ca^{2+} und pH unterhalb des aboralen Ektoderms. Dieser Befund weist darauf hin, dass Ca-ATPase am aboralen Ektoderm Ca^{2+} entgegen dem Gradienten im Austausch mit H^+ transportiert. Zusatz von DCMU, einem Inhibitor des Foto-systems II, bewirkte eine komplette Inhibition der Fotosynthese. Die typische Dynamik der Ca^{2+}-Konzentration unterhalb des aboralen Ektoderms setzte sich jedoch, wenn auch mit verminderter Regelmässigkeit, fort. Auch die anfänglichen Raten wurden aufrecht erhalten. Daraus ergibt sich, dass das Licht selbst und nicht die Energieerzeugung die Calciumauf-nahme steuert, wenngleich für den Prozess Energie benötigt wird, welche hauptsächlich durch Veratmung von Fotosyntheseprodukten zur Verfügung gestellt wird.

In einer dritten Untersuchung (Kapitel 4) wurde die Wechselwirkung zwischen Fotosynthese und Calcifikation im Mikromaßstab mittels Mikrosensoren und Mikroautoradio-grafie untersucht. Im Rahmen der Untersuchung mit dem Titel "Spatial distribution of calci-fication and photosynthesis in the scleractinian coral *Galaxea fascicularis*" wurde festge-stellt, dass die höchsten Raten der Brutto-Fotosynthese (Pg) im Bereich des Gewebes vor-liegen, das die

Septen, die Tentakel und den Bereich der Leibesöffnung umgibt. Niedrigere Raten wurden in den Geweben des Wandbereichs und des Coenosarks gemessen. Inkubation der Kolonien mit Radiotracern (Calcium und Carbonat) ergaben, dass die Verteilung der Calcifikation der der Fotosyntheseaktivität entspricht. Somit werden die hohen Wachstums-raten im Bereich der Polypensepten (, welche die höchsten Raten von Tracereinbau zeigten) unterstützt von den hohen Pg der Symbionten in den benachbarten Gewebebereichen. Während die Einbauraten im Licht insgesamt höher waren als in Dunkelheit, wurde das Verteilungsmuster des Radioisotopeneinbaus durch die Beleuchtung nicht beeinflusst. Dies zeigt, dass es sich bei der Verteilung um eine morphogenetisch kontrollierte Eigenschaft handeln muss, was die enge Beziehung zwischen Calcifikation und Fotosynthese noch betont.

Durch den Nachweis des Einbaus von ^{14}C aus HCO_3^- und auch aus Glucose in das Korallenskelett konnte gezeigt werden, dass sowohl organische als auch anorganische Kohlenstoffquellen für die Calcifikation in Korallen genutzt werden können. Es konnte weiterhin demonstriert werden, dass beide Tracer im Licht bevorzugt in das Gewebe und in geringerem Maße in das Skelett einbaut werden, während keinerlei Inkorporation von ^{45}Ca in das Gewebe stattfindet. Dieser Befund unterstützt die Schlussfolgerung aus Kapitel 2 über den Austausch zwischen den Pools.

Über die Verwendung von abgetöteten Korallen in den Inkubationsexperimenten wurden die Isotopenaustauschraten ermittelt um zu einer verbesserten Einschätzung der durch die Korallen bewirkten Calcifikationsraten zu gelangen. Durch den Einsatz neuartiger mikroanalytischer Techniken (Mikrosensoren und β-Imaging) konnte insgesamt in überzeugender Weise zur Beilegung einer klassischen wissenschaftlichen Debatte über die Kopplung von Fotosynthese und Calcifikation beigetragen werden .

List of Publications

1. **Microsensor Study of Photosynthesis and Calcification in the Scleractinian Coral, *Galaxea fascicularis*: active internal carbon cycle**

   Fuad A. Al-Horani, Salim M. Al-Moghrabi, Dirk de Beer

   Manuscript submitted for publication in J. Experimental Marine Biology and Ecology

2. **Mechanism of calcification and its relation to photosynthesis and respiration in the scleractinian coral *Galaxea fascicularis***

   Fuad A. Al-Horani, Salim M. Al-Moghrabi, Dirk de Beer

   Manuscript submitted for publication in Marine Biology

3. **Spatial distribution of calcification and photosynthesis in the scleractinian coral *Galaxea fascicularis***

   Fuad A. Al-Horani, Tim Ferdelman, Salim M. Al-Moghrabi, Dirk de Beer

   Manuscript submitted for publication in Coral Reefs